Nematic single-component superconductivity and loop-current order from pair-density wave instability

Jonatan Wårdh[*] and Mats Granath [†]
Department of Physics, University of Gothenburg, SE-41296 Gothenburg, Sweden

We investigate the nematic and loop-current-type orders that may arise as vestigial precursor phases in a model with an underlying pair-density wave (PDW) instability. We discuss how such a vestigial phase gives rise to a highly anisotropic stiffness for a coexisting single-component superconductor with low intrinsic stiffness, as is the case for the underdoped cuprate superconductors. Next, focusing on a regime with a mean-field PDW ground state with loop-current and nematic xy (B_{2g}) order, we find a preemptive transition into low- and high-temperature vestigial phases with loop-current and nematic order corresponding to xy (B_{2g}) and $x^2 - y^2$ (B_{1g}) symmetry, respectively. Near the transition between the two phases, a state of soft nematic order emerges for which we expect that the nematic director is readily pinned away from the high-symmetry directions in the presence of an external field. Results are discussed in relation to findings in the cuprates, especially to the recently inferred highly anisotropic superconducting fluctuations [Wårdh *et al.*, arXiv:2203.06769], giving additional evidence for an underlying ubiquitous PDW instability in these materials.

I. INTRODUCTION

One major challenge in the study of cuprate high-temperature superconductors is to unravel the intricate interplay of "intertwined" electronics orders [1], and their relation to the pseudogap. Spin and charge orders have been shown to be ubiquitous phenomena in these compounds [2–5], as well as nematic order [6–10]. Another pertinent electronic order is the spatially modulated superconducting state, known as a pair-density wave (PDW) [11,12], which is conceptually related to the Fulde-Ferrell-Larkin-Ovchinnikov (FFLO)-type [13,14] type states. The PDW came to prominence in the cuprate context to explain the anomalous suppression of superconductivity at 1/8 doping in the striped superconductor $La_{2-x}Ba_xCuO_4$ [2,15–18]. More recently, to explain the apparent residual superconductivity in the pseudogap, in the form of a prevalent diamagnetic response [19], together with the omnipresent charge-density wave (CDW), PDW order has also been suggested as the "mother state" of the pseudogap itself [20,21]. Related to this, PDW has been discussed in the context of Fermi arcs [22], and the anomalous quantum oscillations at large magnetic fields [23–25]. More direct signatures have been reported based on scanning tunneling spectroscopy [26,27]. Furthermore, numerous evidence points towards a time-reversal-symmetry breaking intraunit cell magnetic order present in the pseudogap phase [28–33]. This has spurred the suggestion of various kinds of magnetoelectric (ME) orders, specifically so-called loop-current orders [34–38], which break time-reversal symmetry and parity but preserve their product.

Another recent theme in the physics of strongly correlated materials and the cuprates is that of vestigial orders, which refers to the emergence of a secondary order parameter that breaks a subgroup of symmetries of a multicomponent order parameter at a critical temperature that may surpass that of the underlying order. Such discrete broken symmetry has been discussed both in the context of nematic order [39–41] and broken time-reversal symmetry [42–45], as well as partially broken continuous symmetry phases of multicomponent superconductors [46].

Vestigial order is natural to appeal to as a source for intracell order when the multicomponent order is related to the point group of the lattice and has been studied as a source of nematicity, with evidence in iron-based, topological, and cuprate superconductors [41,47–50]. In hole-doped $Ba_{1-x}K_xFe_2As_2$ a recent study shows evidence for a state with incoherent pairing but broken time-reversal symmetry consistent with a vestigial state of a multiband superconductor [51]. In the cuprates, vestigial-nematic order has been suggested to possibly arise both from spin and charge order [52,53], as well as PDW [54]. It has also been shown that loop-current orders can arise as a vestigial order that preempts a magnetoelectric PDW (ME-PDW) state [54]. In this paper we explore the occurrence and competition between various PDW-vestigial phases, motivated both by an explicit model for stabilizing PDW order based on pair-hopping interactions [55,56] (see also [57]), and by recent experiments on strongly nematic phase fluctuations in a cuprate superconductor [58].

*jonatan.wardh@gmail.com
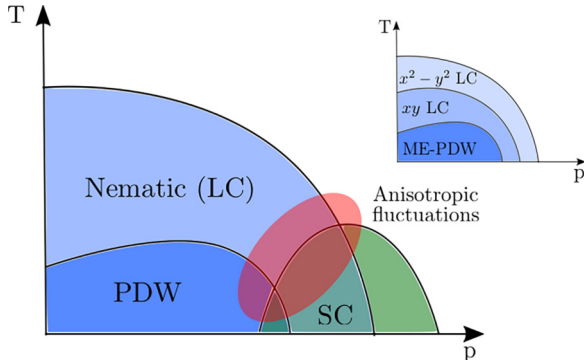†mats.granath@physics.gu.se

FIG. 1. Possible interpretation of cuprate phase diagram with a PDW as the mean-field pseudogap state setting up vestigial nematic as well as loop-current (LC) order. Near and above T_c in the underdoped part of the superconducting (SC) dome, this is consistent with the anisotropic superconducting fluctuations seen in LSCO [58,61], due to the closeness of a PDW instability and presence of nematic order. The inset shows the possibility of splitting the vestigial nematic phase into low- and high-temperature phases of $xy(B_{2g})$ and $x^2 - y^2(B_{1g})$ nematic order, respectively, due to an underlying magnetoelectric PDW (ME-PDW).

First, we show how the relation between PDW and homogeneous superconductivity naturally generates an anisotropic superconducting state in a vestigial nematic PDW phase. In turn, this anisotropy can become strongly enhanced due to low phase stiffness [59,60], which in itself may also be related to a proximate PDW instability [55,56]. Transport measurements in La$_{2-x}$Sr$_x$CuO$_4$ (LSCO) have shown evidence of an electronic nematic order [61]. These measurements indicate highly anisotropic superconducting fluctuations near the underdoped critical point, with only a small anisotropy of the normal electrons [58]. This is consistent with the collective dynamics of the superconductor being highly susceptible to nematic order, along the lines presented in the present paper. A caricature of a phase diagram based on such a scenario, with interplay between superconductivity and vestigial PDW order, is presented in Fig. 1.

In tetragonal symmetry, loop-current (LC) order is associated with a vector $\vec{l} = (l_x, l_y)$, transforming in the E_u representation. In the second part of the paper we will explore a scenario with an underlying ME-PDW state with LC order, which is invariant under reflection in the crystallographic diagonal xy ($l_x = l_y$), with subleading xy (or B_{2g}) nematic order $l_x l_y$. This phase is naturally preempted by a phase without the long-range PDW order but with vestigial LC and nematic order [54], which we refer to as an xy LC phase. We show that this preemptive transition can be split further into low- and high-temperature phases. The low-temperature phase coincides with the xy LC phase, while the high-temperature phase breaks the tetragonal symmetry differently, by developing LC order which is invariant under reflection in the crystallographic axis $l_x \neq 0, l_y = 0$, i.e., $x^2 - y^2$ (or B_{1g}) nematic order $l_x^2 - l_y^2$. We refer to this as an $x^2 - y^2$ LC phase. Besides giving a richer phase diagram with both B_{1g} and B_{2g} symmetric orders, arising from the same underlying ME-PDW state, we find near the first-order transition between the $x^2 - y^2$ and xy LC phases a state with approximate rotational symmetry in $\vec{l}$.

This yields a very soft nematic order that is highly susceptible to external fields that may pin the nematic director away from the high-symmetry directions.

Outline

This paper is composed of two main results parts and is outlined as follows. In Sec. II the considered model is discussed. This model is based on the phenomenology of an instability to a PDW state developed in [55,56], but shares features with other discussed models for a PDW state [21,57,62–64]. In the first results part, Sec. III, the model is decomposed into possible vestigial order parameters which is then used to develop an effective model of a uniform, but anisotropic, superconducting state, Eq. (18). In Sec. III B we discuss how the proximity to a PDW instability, with concomitant vestigial nematic order, can give rise to a very large stiffness anisotropy of the superconductor.

In the second results part, Sec. IV C, we explore the possible vestigial phases to a PDW state, implicitly assumed in Sec. III. Here we focus on a parameter regime where the xy ME-PDW is stable, exploring its potential vestigial phases.

II. MODEL

A PDW state denotes a state where paired electrons have finite momenta $\Delta_{\mathbf{Q}} \sim \langle c_{\downarrow,\mathbf{k}} c_{\uparrow,-\mathbf{k}+\mathbf{Q}} \rangle$. We consider the situation when a PDW state (with a spatially modulated superconducting order) is near degenerate with a homogeneous superconducting state. The partition function takes the form $Z = \int \mathcal{D}\Delta \, e^{-S}$ with

$$S = \frac{1}{T} \int_{\vec{x}} r_0 |\Delta(\vec{x})|^2 + \Delta^*(\vec{x})\varepsilon(\vec{D})\Delta(\vec{x})$$
$$+ \frac{1}{2T} \int_{\substack{\vec{x}_1, \vec{x}_2 \\ \vec{x}_3, \vec{x}_4}} U(\vec{x}_1, \vec{x}_2, \vec{x}_3, \vec{x}_4)\Delta(\vec{x}_1)\Delta^*(\vec{x}_2)\Delta(\vec{x}_3)\Delta^*(\vec{x}_4),$$
$$(1)$$

where $\vec{D} = -i\vec{\nabla} - 2e\vec{A}$. The action S is given by the most general [two-dimensional (2D)] Ginzburg-Landau expression, with interaction U, to fourth order in superconducting order, which respects $U(1)$ gauge symmetry, translational symmetry, and the point-group symmetry D_{4h}. In order to describe an instability towards PDW order the superconducting "dispersion" $\varepsilon(\vec{p})$ should develop minima at finite momenta. We consider a general dispersion to sixth order in momenta $\vec{p} = (p_x, p_y)$,

$$\varepsilon(\vec{p}) = ap^2 + bp_x^2 p_y^2 + c(p^2)^2 + d(p^2)^3 + e(p_x^4 p_y^2 + p_y^4 p_x^2),$$
$$(2)$$

and to ensure stability we take $d > 0$, $e > -4d$. This renormalized dispersion naturally occur in models with pair-hopping interactions [55,56], but can also be considered a phenomenological model for coexisting zero- and finite-momentum superconductivity.

The instability to PDW order can occur in two different ways. The first, as shown in Figs. 2(a)–2(c), is a continuous evolution of the pairing momenta from $p = 0$ to finite p,
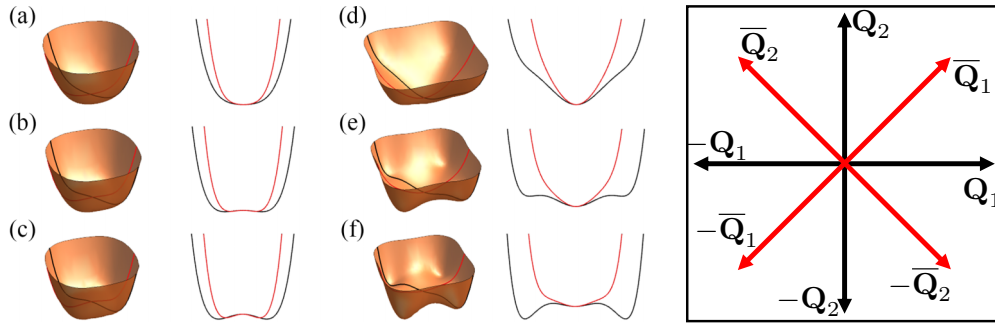
FIG. 2. The dispersion (2) shown for various a and c, and $d > 0$, $e = 0$, $b > 0$. Left: Dispersion along the crystal axis, x, (black), and along the diagonal (red). [(a)–(c)] Successive decrease of a for $c > 0$. A finite q develops continuously from zero. [(d)–(f)] Successive decrease of a for $c < 0$. (d) For big enough a, there is only a stable state at $q = 0$; (e) by decreasing a a metastable $q \neq 0$ state develops, which eventually becomes (f) the new stable state. Right: The corresponding PDW ordering vectors.

parametrized by a going from positive to negative for $c > 0$. When $a = 0$ the dispersion of the homogeneous superconductor becomes flat, constituting a Lifshitz point, where the stiffness to fluctuations goes to zero. The second, occurring when $c < 0$ and shown in Figs. 2(d)–2(f), is a discontinuous jump in p through the development of a distinct metastable state at finite momenta $p \neq 0$, which becomes stable when a is decreased sufficiently. The dispersion (2) allows local minima along both the axes and the diagonals. In general eight finite momentum vectors are allowed, $\pm\mathbf{Q}_1$, $\pm\mathbf{Q}_2$, $\pm\overline{\mathbf{Q}}_1$, and $\pm\overline{\mathbf{Q}}_2$ given by $\mathbf{Q}_1 = Q(1, 0)$, $\mathbf{Q}_2 = Q(0, 1)$, $\overline{\mathbf{Q}}_1 = \overline{Q}(1, 1)/\sqrt{2}$, and $\overline{\mathbf{Q}}_2 = \overline{Q}(-1, 1)/\sqrt{2}$.

In order to analyze the fluctuations near the onset of these finite momentum orders we will go on reexpressing Eq. (1) by expanding in the various finite momentum superconducting order parameters. We will, however, leave the explicit form of the fourth-order term U in Eq. (1) unspecified and instead infer the expansion by considering all symmetry-allowed terms. Before writing down the expression for the expanded action, we first discuss formally what terms are allowed.

A. Symmetry and order parameters

We consider the tetragonal point-group symmetry D_{4h} generated by $\{C_4, \sigma_v, \sigma_h\}$, where C_4 is a fourfold rotation about the z axis, σ_v reflection in the $xz(yz)$ plane, and σ_h reflection in the xy plane. The different momenta of the PDW order lead to eight different complex order parameters, and one ordinary homogeneous superconducting field Δ_0. The latter is assumed to be a single-component complex field, transforming in a one-dimensional representation of the point group, e.g., a $d_{x^2-y^2}$ wave order. The set of order parameters, Γ, is divided into three sectors, A, B, and SC, $\Gamma = \Gamma_A \oplus \Gamma_B \oplus \Delta_0$. $\Gamma_A = \{\Delta_{\mathbf{Q}_1}, \Delta_{-\mathbf{Q}_1}, \Delta_{\mathbf{Q}_2}, \Delta_{-\mathbf{Q}_2}\}$ and $\Gamma_B = \{\Delta_{\overline{\mathbf{Q}}_1}, \Delta_{-\overline{\mathbf{Q}}_1}, \Delta_{\overline{\mathbf{Q}}_2}, \Delta_{-\overline{\mathbf{Q}}_2}\}$ contain the PDW fields and do not transform into each other under D_{4h}, but their form is related by a $45°$ twist. These are denoted by black and red in Fig. 2. Besides the point-group symmetry, the action will be invariant under $U(1)$ gauge symmetry, translational symmetry, and time-reversal symmetry. Under these symmetries the order parameters transform as $\Delta_{\mathbf{Q}} \xrightarrow{U(1)} \Delta_{\mathbf{Q}} e^{i\theta}$, $\Delta_{\mathbf{Q}} \xrightarrow{T} \Delta_{\mathbf{Q}} e^{i\mathbf{T}\cdot\mathbf{Q}}$, and $\Delta_{\mathbf{Q}} \xrightarrow{\mathcal{T}} \Delta_{-\mathbf{Q}}^*$.

1. Composite order parameters

The action will be made up of all possible products of Γ that transform trivially under the full symmetry group $U(1) \otimes T \otimes \mathcal{T} \otimes D_{4h}$. These will be second-order terms, $\Gamma^* \otimes \Gamma$, and fourth-order terms, $\Gamma^* \otimes \Gamma \otimes \Gamma^* \otimes \Gamma$. (Terms including derivatives are discussed in Sec. II A 2.) The possible vestigial phases will be described by a set of order parameters, $\{\phi_1, \phi_2, \dots\}$, which are to second order in the primary fields $\phi \sim \Gamma^* \otimes \Gamma$, and transforming in nontrivial irreducible representations. We reexpress the action in these composite order parameters, integrating out the PDW fields, Γ. The new action will thus be made up of products of these composite order parameters, that transform trivially under the full symmetry group. The breaking of symmetries and emergence of vestigial phases is then understood in the language of a Landau phase transition $L = a\phi^2 + b\phi^4$ where the order parameter ϕ develops a nonzero expectation value for $a < 0$, thus breaking the corresponding symmetry of the system.

We are especially interested in composite orders that only break the point-group symmetries, i.e., nonsuperconducting intraunit cell orders. There are nine bilinears that transform trivially under $U(1) \otimes T$, which we write as $\Gamma^{(2)} = \Gamma_A^{(2)} \oplus \Gamma_B^{(2)} \oplus |\Delta_0|^2$, where $\Gamma_A^{(2)} = \{|\Delta_{\mathbf{Q}_1}|^2, |\Delta_{-\mathbf{Q}_1}|^2, |\Delta_{\mathbf{Q}_2}|^2, |\Delta_{-\mathbf{Q}_2}|^2\}$ and $\Gamma_B^{(2)} = \{|\Delta_{\overline{\mathbf{Q}}_1}|^2, |\Delta_{-\overline{\mathbf{Q}}_1}|^2, |\Delta_{\overline{\mathbf{Q}}_2}|^2, |\Delta_{-\overline{\mathbf{Q}}_2}|^2\}$. Again, $\Gamma_A^{(2)}$ and $\Gamma_B^{(2)}$ do not mix under D_{4h} and can be decomposed further into their irreducible representations, $\Gamma_A^{(2)} = A_{1g} \oplus B_{1g} \oplus E_u$ and $\Gamma_B^{(2)} = A_{1g} \oplus B_{2g} \oplus E_u$, which are listed in Table I.

The decomposition into bilinears implies the existence of two nematic order parameters, transforming as B_{1g} and B_{2g}, as well as two polar vector orders, transforming as E_u. The polar-vector order $l_i = |\Delta_{\mathbf{Q}_i}|^2 - |\Delta_{-\mathbf{Q}_i}|^2$ is odd under parity and has the symmetry of a toroidal moment, which shares symmetry with the so-called loop-current (LC) order, and we will refer to it as such. We will refer to an ME-PDW as a PDW with finite expectation value on LC order.

2. Derivative terms

Derivative terms arise by forming products between $\vec{D} = (D_x, D_y)$ (transforming as E_u) and the bilinears $\Gamma^{(2)}$. For Δ_0, transforming as A_{1g}, no linear derivative terms can arise to

TABLE I. Possible irreducible representations of the set of composite orders (bilinears) $\Gamma^{(2)} = \Gamma_A^{(2)} \oplus \Gamma_B^{(2)} \oplus |\Delta_0|^2$, where $\Gamma_A^{(2)} = \{|\Delta_{\mathbf{Q}_1}|^2, |\Delta_{-\mathbf{Q}_1}|^2, |\Delta_{\mathbf{Q}_2}|^2, |\Delta_{-\mathbf{Q}_2}|^2\}$ and $\Gamma_B^{(2)} = \{|\Delta_{\overline{\mathbf{Q}}_1}|^2, |\Delta_{-\overline{\mathbf{Q}}_1}|^2, |\Delta_{\overline{\mathbf{Q}}_2}|^2, |\Delta_{-\overline{\mathbf{Q}}_2}|^2\}$.

Bilinears	Irreducible representations
$|\Delta_0|^2$	A_{1g}, z^2
$\psi_B : |\Delta_{\mathbf{Q}_1}|^2 + |\Delta_{-\mathbf{Q}_1}|^2 + |\Delta_{\mathbf{Q}_2}|^2 + |\Delta_{-\mathbf{Q}_2}|^2$	A_{1g}, x^2+y^2
$N_{x^2-y^2} : |\Delta_{\mathbf{Q}_1}|^2 + |\Delta_{-\mathbf{Q}_1}|^2 - |\Delta_{\mathbf{Q}_2}|^2 - |\Delta_{-\mathbf{Q}_2}|^2$	B_{1g}, x^2-y^2
$\vec{l}_A : [|\Delta_{\mathbf{Q}_1}|^2 - |\Delta_{-\mathbf{Q}_1}|^2, |\Delta_{\mathbf{Q}_2}|^2 - |\Delta_{-\mathbf{Q}_2}|^2]$	$E_u, (x, y)$
$\psi_A : |\Delta_{\overline{\mathbf{Q}}_1}|^2 + |\Delta_{-\overline{\mathbf{Q}}_1}|^2 + |\Delta_{\overline{\mathbf{Q}}_2}|^2 + |\Delta_{-\overline{\mathbf{Q}}_2}|^2$	A_{1g}, x^2+y^2
$N_{xy} : |\Delta_{\overline{\mathbf{Q}}_1}|^2 + |\Delta_{-\overline{\mathbf{Q}}_1}|^2 - |\Delta_{\overline{\mathbf{Q}}_2}|^2 - |\Delta_{-\overline{\mathbf{Q}}_2}|^2$	B_{2g}, xy
$\vec{l}_B : \left[\dfrac{|\Delta_{\overline{\mathbf{Q}}_1}|^2 - |\Delta_{-\overline{\mathbf{Q}}_1}|^2 - |\Delta_{\overline{\mathbf{Q}}_2}|^2 + |\Delta_{-\overline{\mathbf{Q}}_2}|^2}{\sqrt{2}}, \dfrac{|\Delta_{\overline{\mathbf{Q}}_1}|^2 - |\Delta_{-\overline{\mathbf{Q}}_1}|^2 + |\Delta_{\overline{\mathbf{Q}}_2}|^2 - |\Delta_{-\overline{\mathbf{Q}}_2}|^2}{\sqrt{2}} \right]$	$E_u, (x, y)$

any order in Δ_0. Mixing with PDW bilinears, transforming as $2A_{1g} \oplus B_{1g} \oplus B_{2g} \oplus 2E_u$, linear derivatives are allowed both to second and fourth order in fields. But, terms linear in derivatives imply an instability of the PDW momenta. Thus, expanding around stable local minima of Eq. (2) will to first nonvanishing order generate second-order terms in derivative and fields.

We do have the possibility of including derivative terms that are to fourth order in fields. However, usually these terms are irrelevant compared to derivative terms arising to second order in fields. We will assume this is still true for the PDW fields, for which these terms will be neglected. However, near the Lifshitz point, where the dispersion for Δ_0 becomes flat, derivative terms acting on Δ_0, occurring to fourth order in fields, will be important to include. To second order in derivatives and to fourth order in fields, we can form products between an A_{1g} derivative term and the A_{1g} bilinears, or the B_{1g} (B_{2g}) derivative term with the B_{1g} (B_{2g}) bilinears. The first term contributes to the isotropic stiffness and is of no particular interest (it can be included in the overall renormalization); the second type of term will, however, generate an anisotropic stiffness in the presence of (vestigial) nematic order from the PDW fields.

Terms linear in derivative do occur by coupling to the E_u bilinears. This coupling will shift the zero momentum Δ_0 in the presence of LC. But as long as the dispersion is well approximated with a parabola, this shift will not change the dispersion around the stable point, and the response will remain isotropic. Therefore, we will neglect these terms even in the presence of LC order.

B. Expanded action

We find the expanded action (1) in terms of the irreducible representation discussed above as $S = S_{\text{PDW}} + S_0 + S_{\text{PDW}-0}$, where S_0 contains the homogeneous superconducting field

$$S_0 = \int_{\vec{x}} \kappa |\vec{D}\Delta_0|^2 + r_0|\Delta_0|^2 + \frac{u}{2}|\Delta_0|^4, \qquad (3)$$

S_{PDW} the PDW fields, and $S_{\text{PDW}-0}$ their interaction. S_{PDW} can be divided further, $S_{\text{PDW}} = S_A + S_B + S_{A-B}$, one for each sector, respectively, which will take the same form, but with independent parameters:

$$S_A = \int_{\vec{x}} \sum_{\mathbf{q}=\pm\mathbf{Q}_{1,2}} \kappa_1 |\vec{D}\Delta_{\mathbf{q}}|^2 + \kappa_2 \left[\sum_{\mathbf{q}=\pm\mathbf{Q}_1} (|D_x\Delta_{\mathbf{q}}|^2 - |D_y\Delta_{\mathbf{q}}|^2) - \sum_{\mathbf{q}=\pm\mathbf{Q}_2} (|D_x\Delta_{\mathbf{q}}|^2 - |D_y\Delta_{\mathbf{q}}|^2) \right] + \sum_{\mathbf{q}=\pm\mathbf{Q}_{1,2}} r|\Delta_{\mathbf{q}}|^2 + \frac{u_0}{2}|\Delta_{\mathbf{q}}|^4$$

$$+ \frac{u_1}{2}[|\Delta_{\mathbf{Q}_1}|^2 + |\Delta_{-\mathbf{Q}_1}|^2 - |\Delta_{\mathbf{Q}_2}|^2 - |\Delta_{-\mathbf{Q}_2}|^2]^2 + \frac{u_2}{2}[(|\Delta_{\mathbf{Q}_1}|^2 - |\Delta_{-\mathbf{Q}_1}|^2)^2 + (|\Delta_{\mathbf{Q}_2}|^2 - |\Delta_{-\mathbf{Q}_2}|^2)^2],$$

$$S_{A-B} = \int_{\vec{x}} v_0 \left[\sum_{\mathbf{q}=\pm\mathbf{Q}_{1,2}} |\Delta_{\mathbf{q}}|^2 \right] \left[\sum_{\mathbf{q}'=\pm\overline{\mathbf{Q}}_{1,2}} |\Delta_{\mathbf{q}'}|^2 \right] + \frac{v_1}{\sqrt{2}} (|\Delta_{\mathbf{Q}_1}|^2 - |\Delta_{-\mathbf{Q}_1}|^2, |\Delta_{\mathbf{Q}_2}|^2 - |\Delta_{-\mathbf{Q}_2}|^2)$$

$$\times (|\Delta_{\overline{\mathbf{Q}}_1}|^2 - |\Delta_{-\overline{\mathbf{Q}}_1}|^2 - |\Delta_{\overline{\mathbf{Q}}_2}|^2 + |\Delta_{-\overline{\mathbf{Q}}_2}|^2, |\Delta_{\overline{\mathbf{Q}}_1}|^2 - |\Delta_{-\overline{\mathbf{Q}}_1}|^2 + |\Delta_{\overline{\mathbf{Q}}_2}|^2 - |\Delta_{-\overline{\mathbf{Q}}_2}|^2),$$

$$S_{\text{PDW}-0} = \int_{\vec{x}} \gamma_0 |\Delta_0|^2 \left[\sum_{\mathbf{q}=\pm\mathbf{Q}_{1,2}} |\Delta_{\mathbf{q}}|^2 \right] + \gamma_1 (|D_x\Delta_0|^2 - |D_y\Delta_0|^2)(|\Delta_{\mathbf{Q}_1}|^2 + |\Delta_{-\mathbf{Q}_1}|^2 - |\Delta_{\mathbf{Q}_2}|^2 - |\Delta_{-\mathbf{Q}_2}|^2), \qquad (4)$$

where we absorbed a factor $1/T$ in all coefficients. As stated previously, the coefficients could be traced back to the exact form of the full Ginzburg-Landau model, Eq. (1), but we will consider them as independent parameters [65].

S_B has the same form as S_A with $\mathbf{Q}_{1,2} \to \overline{\mathbf{Q}}_{1,2}$ and $x, y \to \overline{x}, \overline{y}$ where $\overline{x} = \frac{x+y}{\sqrt{2}}, \overline{y} = \frac{-x+y}{\sqrt{2}}$. When in need of specifying both sectors we will append the subscript A or B to r, u_0, u_1, u_2, γ_0, and γ_1. The second-order term coefficients r, r_0 are assumed to be proportional to the temperature T, changing sign at the mean-field transition temperature $r \propto T - T_{\text{PDW}}$, $r_0 \propto T - T_{\text{SC}}$.

The interaction of the two sectors S_{A-B} occurs in fourth-order terms and only involves the A_{1g} and E_u representation of both sectors. Throughout the text, we will only explicitly assume a stable A sector, meaning that Eq. (2) only supports local minima of momenta along the axis, for which S_B and S_{A-B} drop out. However, we will reinsert the B sector when the result is directly generalizable. Discussion regarding the inclusion of both the A and B sectors is found in Appendix E. As mentioned above, we have left out terms consisting of bilinears that transform nontrivially under $U(1)$: Δ_0^2, $(\Delta_{\mathbf{Q}_1}\Delta_{-\mathbf{Q}_1} \pm \Delta_{\mathbf{Q}_2}\Delta_{-\mathbf{Q}_2})$, $(\Delta_{\overline{\mathbf{Q}}_1}\Delta_{-\overline{\mathbf{Q}}_1}$

$\pm \Delta_{\overline{\mathbf{Q}}_2}\Delta_{-\overline{\mathbf{Q}}_2}$). These secondary order parameters refer to so-called 4e superconducting order [66], which we neglect in subsequent analysis.

III. EFFECTIVE ANISOTROPIC SUPERCONDUCTOR

Now we will discuss the fate of the superconducting order in the presence of PDW vestigial order without any specific assumptions about the underlying instability or parameter regime. (Exploration of the ME-PDW vestigial phases is left for Sec. IV.) In the absence of long-range PDW order, $\langle \Delta_{\mathbf{Q}} \rangle = 0$, it is straightforward to integrate the PDW fields out, leaving an action only dependent on the vestigial order parameters and SC Δ_0.

We begin by promoting the secondary order parameters to independent fields, which we do by decoupling the fourth-order terms in Eqs. (4) using the Hubbard-Stratonovich

transformation,

$$e^{-\int_{\bar{x}} \Phi^* \frac{M}{2} \Phi} = \int \mathcal{D}\Psi\, e^{\int_{\bar{x}} \Psi^* \frac{M^{-1}}{2}\Psi - \Phi^* \cdot \Psi}. \tag{5}$$

Here Φ is a vector of the bilinears listed in Table I and Ψ the corresponding vector of the auxiliary field to decouple that bilinear. The matrix M is inferred from Eqs. (4) and contains the coupling constants. We will assume only a stable A sector, yielding a diagonal M. We denote the auxiliary fields with $\psi, N_{x^2-y^2}, \vec{l}$, dropping the index A, corresponding to the bilinear they decouple (see Table I). Using this transformation, we express the partition function as

$$Z = \int \mathcal{D}\{\Delta_{\mathbf{Q}}\}\mathcal{D}\Delta_0 \mathcal{D}\{\psi, N_{x^2-y^2}, \vec{l}\}\, e^{-S_{\text{eff}}}, \tag{6}$$

with the effective action given by

$$
\begin{aligned}
&S_{\text{eff}}(\{\Delta_{\mathbf{Q}}\}, \Delta_0, \psi, N_{x^2-y^2}, \vec{l}) \\
&= \int_{\bar{k}} \chi_0^{-1}(k)|\Delta_0|^2 + \frac{u}{2}|\Delta_0|^4 + \chi_x^{-1}(\vec{k})\big(|\Delta_{\mathbf{Q}_1}|^2 + |\Delta_{-\mathbf{Q}_1}|^2\big) + \chi_y^{-1}(\vec{k})\big(|\Delta_{\mathbf{Q}_2}|^2 + |\Delta_{-\mathbf{Q}_2}|^2\big) \\
&\quad + \int_{\vec{x}} (\psi + \gamma_0|\Delta_0|^2)\big(|\Delta_{\mathbf{Q}_1}|^2 + |\Delta_{-\mathbf{Q}_1}|^2 + |\Delta_{\mathbf{Q}_2}|^2 + |\Delta_{-\mathbf{Q}_2}|^2\big) + l_x\big(|\Delta_{\mathbf{Q}_1}|^2 - |\Delta_{-\mathbf{Q}_1}|^2\big) + l_y\big(|\Delta_{\mathbf{Q}_2}|^2 - |\Delta_{-\mathbf{Q}_2}|^2\big) \\
&\quad + \int_{\vec{x}} \big(N_{x^2-y^2} + \gamma_1(|D_x\Delta_0|^2 - |D_y\Delta_0|^2)\big)\big(|\Delta_{\mathbf{Q}_1}|^2 + |\Delta_{-\mathbf{Q}_1}|^2 - |\Delta_{\mathbf{Q}_2}|^2 - |\Delta_{-\mathbf{Q}_2}|^2\big) - \left(\frac{\psi^2}{2u_0} + \frac{N_{x^2-y^2}^2}{2u_1} + \frac{\vec{l}^2}{2u_2}\right), \tag{7}
\end{aligned}
$$

where $\chi_0^{-1} = r_0 + \kappa(k_x^2 + k_y^2)$ and $\chi_{x,y}^{-1} = r + \kappa_1(k_x^2 + k_y^2) \pm \kappa_2(k_x^2 - k_y^2)$. We have left out the gauge field $\vec{A}$ (absorbing it in the phase gradient), considering an extreme type-II superconductor, for which the electromagnetic field energy can be ignored. We will treat $\psi, N_{x^2-y^2}, \vec{l}$ on a mean-field level and only keep the uniform component (i.e., $\psi(\vec{q}) = \psi(2\pi)^d\delta(\vec{q})$, etc.). The composite field ψ will always have a nonzero and positive expectation value since it describes the fluctuations of the PDW state,

$$\frac{\psi}{u_0} = \int_{\vec{x}} \langle |\Delta_{\mathbf{Q}_1}|^2 + |\Delta_{-\mathbf{Q}_1}|^2 + |\Delta_{\mathbf{Q}_2}|^2 + |\Delta_{-\mathbf{Q}_2}|^2 \rangle, \tag{8}$$

and is, therefore, not an order parameter. Similarly, developing a nonzero expectation value on any of the vestigial-order parameters implies

$$
\begin{aligned}
\frac{N_{x^2-y^2}}{u_1} &= \int_{\vec{x}} \langle |\Delta_{\mathbf{Q}_1}|^2 + |\Delta_{-\mathbf{Q}_1}|^2 - |\Delta_{\mathbf{Q}_2}|^2 - |\Delta_{-\mathbf{Q}_2}|^2 \rangle, \\
\frac{l_x}{u_2} &= \int_{\vec{x}} \langle |\Delta_{\mathbf{Q}_1}|^2 - |\Delta_{-\mathbf{Q}_1}|^2 \rangle, \\
\frac{l_y}{u_2} &= \int_{\vec{x}} \langle |\Delta_{\mathbf{Q}_2}|^2 - |\Delta_{-\mathbf{Q}_2}|^2 \rangle, \tag{9}
\end{aligned}
$$

respectively. Even in absence of PDW order we find nonequivalent uniform static susceptibilities once the vestigial order

parameters $N_{x^2-y^2}, \vec{l}$ are finite:

$$
\begin{aligned}
\chi_{\mathbf{Q}_1}(0) &= \frac{1}{r' + N_{x^2-y^2} + l_x}, & \chi_{-\mathbf{Q}_1}(0) &= \frac{1}{r' + N_{x^2-y^2} - l_x}, \\
\chi_{\mathbf{Q}_2}(0) &= \frac{1}{r' - N_{x^2-y^2} + l_y}, & \chi_{-\mathbf{Q}_2}(0) &= \frac{1}{r' - N_{x^2-y^2} - l_y}, \tag{10}
\end{aligned}
$$

where $r' = r + \gamma_0|\Delta_0|^2 + \psi$ [see Eqs. (24) for the full static susceptibilities]. Without vestigial ordering, the transition temperature would be given by $r' = 0$. Thus we see a splitting of the transition into the ordered PDW state and that the preemptive transition enhances the transition temperature.

A. Superconducting action

The effective action (7) can be written in the form

$$
\begin{aligned}
&S_{\text{eff}}(\{\Delta_{\mathbf{Q}}\}, \Delta_0, \psi, N_{x^2-y^2}, \vec{l}) \\
&= -V\left(\frac{\psi^2}{2u_0} + \frac{N_{x^2-y^2}^2}{2u_1} + \frac{\vec{l}^2}{2u_2}\right) + \int_k \chi_0^{-1}(k)|\Delta_0|^2 \\
&\quad + \int_r \frac{u}{2}|\Delta_0|^4 + \int_k [\Delta_{\mathbf{Q}_1}\Delta_{-\mathbf{Q}_1}\Delta_{\mathbf{Q}_2}\Delta_{-\mathbf{Q}_2}]_i^* \\
&\quad \times \mathcal{G}_i^{-1}[\Delta_{\mathbf{Q}_1}\Delta_{-\mathbf{Q}_1}\Delta_{\mathbf{Q}_2}\Delta_{-\mathbf{Q}_2}]_i, \tag{11}
\end{aligned}
$$

where V is the volume, and we have moved to momentum representation.

The kernel $\mathcal{G}$ is given by

$$
\begin{aligned}
\mathcal{G}_1^{-1}(k) &= \chi_x^{-1}(k) + \psi + N_{x^2-y^2} + l_x + \Gamma_x, \\
\mathcal{G}_2^{-1}(k) &= \chi_x^{-1}(k) + \psi + N_{x^2-y^2} - l_x + \Gamma_x, \\
\mathcal{G}_3^{-1}(k) &= \chi_y^{-1}(k) + \psi - N_{x^2-y^2} + l_y + \Gamma_y, \\
\mathcal{G}_4^{-1}(k) &= \chi_y^{-1}(k) + \psi - N_{x^2-y^2} - l_y + \Gamma_y.
\end{aligned}
\tag{12}
$$

Integrating over the PDW fields in Eq. (7) we arrive at the effective action for the vestigial and homogeneous superconducting fields alone:

$$
e^{-S_{\mathrm{eff}}(\Delta_0, \psi, N_{x^2-y^2}, \vec{l})} = \int \mathcal{D}\{\Delta_{\mathbf{Q}}\} e^{-S_{\mathrm{eff}}(\{\Delta_{\mathbf{Q}}\}, \Delta_0, \psi, N_{x^2-y^2}, \vec{l})}. \tag{13}
$$

The new action takes the form

$$
\begin{aligned}
&S_{\mathrm{eff}}(\Delta_0, \psi, N_{x^2-y^2}, \vec{l}) \\
&= -V\left(\frac{\psi^2}{2u_0} + \frac{N_{x^2-y^2}^2}{2u_1} + \frac{\vec{l}^2}{2u_2}\right) \\
&\quad + \int_{\vec{k}} \chi_0^{-1}(\vec{k})|\Delta_0|^2 + \int_{\vec{x}} \frac{u}{2}|\Delta_0|^4 \\
&\quad + V\int_{\vec{k}} \ln\left[\left((\chi_x^{-1}(\vec{k}) + \psi + N_{x^2-y^2} + \Gamma_x)^2 - l_x^2\right)\right. \\
&\quad \left.\times \left((\chi_y^{-1}(\vec{k}) + \psi - N_{x^2-y^2} + \Gamma_y)^2 - l_y^2\right)\right],
\end{aligned}
\tag{14}
$$

where

$$
\Gamma_{x,y} = \frac{\gamma_0}{V}\int_{\vec{k}} |\Delta_0(\vec{k})|^2 \pm \frac{\gamma_1}{V}\int_{\vec{k}} (k_x^2 - k_y^2)|\Delta_0(\vec{k})|^2 \tag{15}
$$

are functionals of the superconducting field. We expand the action in ψ, $N_{x^2-y^2}$, $\vec{l}$, and Δ_0 around their mean-field values [see Eqs. (23)],

$$
S_{\mathrm{eff}}(\Delta_0, \psi, N_{x^2-y^2}, \vec{l}) \approx S_0 + S_{\mathrm{SC}}(\Delta_0), \tag{16}
$$

where $S_0 = S_{\mathrm{eff}}|_{\mathrm{MF}}$ is the action at the mean-field solution, and S_{SC} the effective superconducting action. Above the superconducting transition temperature ($\langle \Delta_0 \rangle = 0$) we find

$$
\begin{aligned}
S_0/V &= -\left(\frac{\psi^2}{2u_0} + \frac{N_{x^2-y^2}^2}{2u_1} + \frac{\vec{l}^2}{2u_2}\right) \\
&\quad + \int_{\vec{k}} \ln\left[\left((\chi_x^{-1}(\vec{k}) + \psi + N_{x^2-y^2})^2 - l_x^2\right)\right. \\
&\quad \left.\times \left((\chi_y^{-1}(\vec{k}) + \psi - N_{x^2-y^2})^2 - l_y^2\right)\right].
\end{aligned}
\tag{17}
$$

In real space the effective superconducting action takes the form

$$
S_{\mathrm{SC}}(\Delta_0) = \int_{\vec{x}} r_0'|\Delta_0(\vec{x})|^2 + \left(\frac{1}{2m_{\mathrm{p}}}\right)_{ij}(D_i\Delta_0(\vec{x}))(D_j\Delta_0(\vec{x}))^*,
$$

$$
\left(\frac{1}{2m_{\mathrm{p}}}\right)_{ij} = \frac{\delta_{ij}}{2m_{\mathrm{p,0}}} + S_{ij}, \quad S = \begin{bmatrix} \frac{\gamma_{1,\mathrm{A}}}{u_{1,\mathrm{A}}} N_{x^2-y^2} & \frac{\gamma_{1,\mathrm{B}}}{u_{1,\mathrm{B}}} N_{xy} \\ \frac{\gamma_{1,\mathrm{B}}}{u_{1,\mathrm{B}}} N_{xy} & -\frac{\gamma_{1,\mathrm{A}}}{u_{1,\mathrm{A}}} N_{x^2-y^2} \end{bmatrix}.
\tag{18}
$$

Here we have reintroduced both the A and B sectors and used the mean-field equations (23) to identify the order parameters. (The mean-field equations for the two primary nematic orders

remain unaltered even in the presence of both A and B sectors; see Appendix E.)

The superconducting effective action (18) is expressed in terms of an anisotropic pair mass [with $\kappa = (2m_{\mathrm{p,0}})^{-1}$], induced by the nematic order parameters through the trace-less symmetric matrix S. (Here we have only explicitly included the primary nematic fields, that are linear in the PDW fluctuations $|\Delta_{\mathbf{Q}}|^2$.) This anisotropic pair mass is equivalent to an anisotropic stiffness, that may be observed, for example, as an anisotropy of the in-plane penetration depth in the superconducting state, or through an anisotropy of the near-T_c normal state conductivity due to superconducting fluctuations [58].

The coupling $r_0' = r_0 + \frac{\gamma_{0,\mathrm{A}}}{u_{0,\mathrm{A}}}\psi_A + \frac{\gamma_{0,\mathrm{A}}}{u_{0,\mathrm{B}}}\psi_B$ is the renormalized inverse static susceptibility. Since Δ_0 is single component, and its amplitude is rotationally symmetric, it cannot couple directly to the nematic order, as seen from the fact that only the symmetric PDW fluctuations $\psi_{A/B}$ contribute. As discussed in Sec. II A 2, expression (18) is expected to hold even in the presence of LC order, although the superconductor would acquire a small finite momentum.

B. Enhancement of anisotropic superconducting fluctuations near PDW instability

In Eqs. (18) we have found an effective superconducting action, renormalized by the PDW fluctuations and the possible vestigial nematic order parameters N_{xy} and $N_{x^2-y^2}$. Note that the superconductor is anisotropic in its dynamics, and, at this level, the static order parameter is still isotropic. However, in the ordered SC state, the nematic order will affect the order parameter. In assuming d-wave superconductivity, there is a coupling $\Delta_d \Delta_s^* N_{x^2-y^2} + \mathrm{H.c.}$ (not considered here), which will induce a subleading s-wave component, effectively shifting the gap nodes. Nevertheless, as we argue below, for a superconductor with low phase stiffness, the effect of even a weak nematic field on the fluctuations may be dramatic, even though the effect on the static gap may be small.

As a digression, we note that this scenario of the effect of vestigial nematic order from superconducting fluctuations on the superconductor is similar in spirit but also different from electron-doped $\mathrm{Bi}_2\mathrm{Se}_3$. The latter has a multicomponent SC order parameter, which may itself form a vestigial nematic phase, which in turn would also affect the dynamics in the normal state [67]. In our case, instead, it is the finite momentum (PDW) superconducting components that give rise to the vestigial nematic order.

One way to probe the anisotropic stiffness of the superconductor is to study the contribution to the conductivity from superconducting fluctuations above T_c, the paraconductivity. At T_c, this contribution will diverge, reflecting the lifetime of Cooper pairs, and we expect to see a strong signature of the nematic order near T_c. As derived in [58], the Aslamazov-Larkin expression for the in-plane paraconductivity of a layered superconductor (interlayer distance d) with anisotropic stiffness is given by

$$
\begin{aligned}
\overline{\sigma}_{\mathrm{p}} &= \frac{e^2}{16\hbar d}\frac{1}{(T/T_c)-1}\sqrt{\det(\overline{m}_{\mathrm{p}})}\,\overline{m}_{\mathrm{p}}^{-1} \\
&\underset{\mathrm{princ.}}{=} \frac{e^2}{16\hbar d}\frac{1}{(T/T_c)-1}\begin{bmatrix} \sqrt{m_{\mathrm{p},b}/m_{\mathrm{p},a}} & 0 \\ 0 & \sqrt{m_{\mathrm{p},a}/m_{\mathrm{p},b}} \end{bmatrix},
\end{aligned}
\tag{19}
$$

where a, b refer to the principal axes of the conductivity, such that the last expression holds in the principal frame. Given a nematic distortion, in the form of Eqs. (18), the pair-mass quotient is given by

$$\frac{m_{p,b}}{m_{p,a}} = \frac{1/2m_{p,0} + \sqrt{S_{xx}^2 + S_{xy}^2}}{1/2m_{p,0} - \sqrt{S_{xx}^2 + S_{xy}^2}}, \qquad (20)$$

where the angle of the a axis (corresponding to the axis of highest conductivity) to the crystal x axis is given by

$$\theta = \arctan \frac{\sqrt{S_{xx}^2 + S_{xy}^2} - S_{xx}}{S_{xy}}. \qquad (21)$$

Thus, in the presence of both N_{xy} (i.e., $S_{xy} \neq 0$) and $N_{x^2-y^2}$ (i.e., $S_{xx} \neq 0$) the principal axes of conductivity will not be aligned with the symmetry axes of the crystal, and will rotate if the relative amplitude of the two fields changes with temperature.

There is, in fact, evidence for highly anisotropic superconducting fluctuations in transport measurements done on thin films of underdoped LSCO [58,61,68], consistent with a high pair-mass ratio $m_{p,b}/m_{p,a}$. This ratio increases as the underdoped critical point is approached, while the quotient of normal masses m_b/m_a remains near 1 [58]. The crystals show very weak signs of lattice distortion, remaining effectively tetragonal, which is in line with the development of electronic nematicity coupling directly to the superconductor, and not through strain [61,68], consistent with the anisotropic superconductor described in Eqs. (18). In addition, the principal axes of the paraconductivity (seen close to T_c) and the normal conductivity are in general not aligned with each other, or with the crystal axes, which is consistent with the presence of both B_{1g} and B_{2b} nematic order.

Nevertheless, the analysis leading up to Eqs. (18) does not by itself explain why the superconducting stiffness anisotropy would be enhanced compared to other observables that couple to nematicity, such as the normal electron conductivity, orthorhombic lattice distortions, and the superconducting gap (as discussed above). However, a natural explanation for this is evident in the expression for the pair-mass ratio (20): if the isotropic pair mass $m_{p,0}$ is sufficiently large (i.e., stiffness small), the quotient $m_{p,b}/m_{p,a}$ will become large even for a small nematic tensor S. Without an explicit microscopic model of how the nematic order couples to normal and paired electrons this is only a qualitative statement, but that the phase stiffness is small in the underdoped cuprates is well established [59].

In fact, proximity to a PDW instability provides a unified conceptual framework in which both the low stiffness and the more recently observed nematic distortion thereof can be understood. As discussed in Sec. II, and more detailed in [56], such an instability is expected to influence also the uniform component by deforming the spectrum of superconducting fluctuations giving a large effective pair mass. In other words, the availability of low-energy finite momentum pair excitations suppresses the stiffness to real-space deformations. Also, as we will further elucidate in the next section, the fluctuations of a (metastable) PDW state can generate vestigial nematic
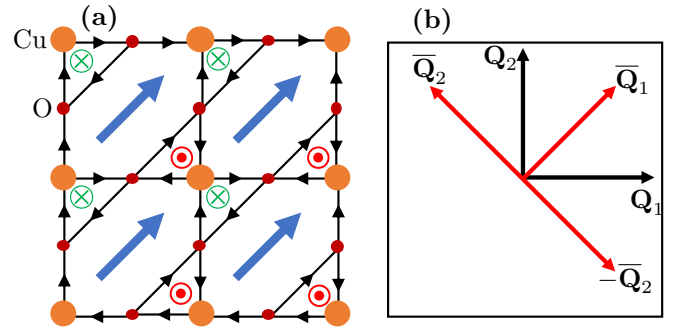

FIG. 3. (a) A loop-current state with microscopic circulating currents suggested to account for the observed time-reversal symmetry seen in cuprates (the so-called Θ_2 state) [28,35]. The LC order is shown as a blue arrow. (b) The corresponding xy ME-PDW state. Black arrows correspond to stable *axial* PDW components, referred to as the A sector, while red arrows show an alternative configuration for stable *diagonal* PDW components (B sector).

order that acts to deform the stiffness. Thus, approaching the finite momentum instability provides a mechanism for generating highly anisotropic superconducting fluctuations, both through creating a low phase stiffness, yielding a high susceptibility towards an anisotropic distortion, as well as providing the distortion itself. This scenario is depicted in Fig. 1, where the pseudogap is made up of vestigial phases set up by an underlying PDW state (possibly ME-PDW, as discussed in the following sections), with anisotropic superconducting fluctuations.

IV. INTERTWINED NEMATIC AND LOOP-CURRENT ORDERS IN THE VESTIGIAL ME-PDW PHASE

In this section we will investigate the various possible vestigial phases from an action of the form (4). Specifically we are interested in the nature of generation of the nematic order coupling to the dynamic response of the homogeneous superconductor through the action (18).

The ME-PDW state argued to be consistent with polarized angle-resolved photoemission spectroscopy measurements [28] has xy LC order corresponding to $(\Delta_{\mathbf{Q}_1}, \Delta_{-\mathbf{Q}_1}, \Delta_{\mathbf{Q}_2}, \Delta_{-\mathbf{Q}_2}) = (\Delta, 0, \Delta, 0)$, which we will refer to as xy ME-PDW. In Fig. 3(a) the PDW momenta for the xy ME-PDW state is shown alongside its circulating current analog [35]. As a speculative scenario for the cuprates, we will consider ME-PDW as a mean-field ground state for the pseudogap phase. The overall stability of action (4) requires $u_0 > 0$. When $u_1 > 0$, $u_2 > 0$, no point-group symmetry is broken. For $u_1 < 0$ we have the possibility for nematic order without LC order, while $u_2 < 0$ is necessary for LC order. The mean-field solutions of S_A in Eq. (4) and the corresponding stable vestigial phase for $u_2 < 0$, $u_1 > 0$ are presented in Table II. Here and subsequently, we use the notation

$$\alpha = \frac{u_0}{|u_2|}, \qquad \beta = \frac{u_1}{|u_2|}, \qquad (22)$$

which parametrize the relative repulsion strength of fluctuation and primary nematic field. [The stability of action (4) requires $\alpha > 0.5$ for $\beta > 0.5$ and $\alpha > 1 - \beta$ for $\beta < 0.5$.]

TABLE II. ME-PDW mean-field ground and first excited states for S_A in Eq. (4) alongside the possible vestigial phases and the corresponding transition order. Here $r < 0$, $\alpha = \frac{u_0}{|u_2|}$, and $\beta = \frac{u_1}{|u_2|}$. States are expressed in the form $(\Delta_{\mathbf{Q}_1}, \Delta_{-\mathbf{Q}_1}, \Delta_{\mathbf{Q}_2}, \Delta_{-\mathbf{Q}_2})$ together with their subleading nematic order. $(\Delta, 0, \Delta, 0)$ corresponds to the xy ME-PDW state. [An equivalent table holds for sector B for $(\Delta_{\overline{\mathbf{Q}}_1}, \Delta_{-\overline{\mathbf{Q}}_1}, \Delta_{\overline{\mathbf{Q}}_2}, \Delta_{-\overline{\mathbf{Q}}_2})$ and $xy \leftrightarrow x^2 - y^2$.] The stability of the vestigial phases assumes a sufficiently low temperature (R) (see Fig. 4). The transition order refers to the vestigial-to-normal phase transition. For $0.5 < \beta < 1$, $\beta < \alpha$, the transition order between the low- and high-temperature phases is first order.

Parameter regime	PDW ground state Nematic order (subleading)	PDW first excited state Nematic order (subleading)	Stable vestigial phase	Transition order from normal state	
$0 < \beta < 0.25$, $1-\beta < \alpha$	$(\Delta, 0, 0, 0)$ $x^2 - y^2$	$(\Delta, 0, \Delta, 0)$ xy	$x^2 - y^2$ LC	first	
$0.25 < \beta < 0.5$, $1-\beta < \alpha < \frac{\beta}{4\beta-1}$	$(\Delta, 0, 0, 0)$ $x^2 - y^2$	$(\Delta, 0, \Delta, 0)$ xy	$x^2 - y^2$ LC	first	
$0.25 < \beta < 0.5$, $\frac{\beta}{4\beta-1} < \alpha$	$(\Delta, 0, \Delta', \Delta')$ $x^2 - y^2$	$(\Delta, 0, 0, 0)$ $x^2 - y^2$	$x^2 - y^2$ LC	$\frac{\beta}{4\beta-1} < \alpha < \frac{2+\beta}{4\beta-1}$ $\frac{2+\beta}{4\beta-1} < \alpha$	first second
$0.5 < \beta < 1$, $0.5 < \alpha < \beta$	$(\Delta, 0, \Delta, 0)$ xy	$(\Delta, 0, \Delta', \Delta')$ $x^2 - y^2$	xy LC	first	
$0.5 < \beta < 1$, $\beta < \alpha$	$(\Delta, 0, \Delta, 0)$ xy	$(\Delta, 0, \Delta', \Delta')$ $x^2 - y^2$	$\left(\begin{array}{c}\text{Low temperature, } xy \text{ LC} \\ \text{High temperature, } x^2 - y^2 \text{LC}\end{array}\right)$	$\beta < \alpha < \frac{2+\beta}{4\beta-1}$ $\frac{2+\beta}{4\beta-1} < \alpha$	first second
$1 < \beta$, $0.5 < \alpha$	$(\Delta, 0, \Delta, 0)$ xy	$(\Delta, 0, \Delta', \Delta')$ $x^2 - y^2$	xy LC	$0.5 < \alpha < 1$ $1 < \alpha$	first second

The mean-field state breaks both continuous $U(1)$ gauge symmetry and the discrete point-group symmetry simultaneously. In the vestigial phase, the point-group symmetry breaking preempts the continuous symmetry breaking. Given that fluctuations act to restore the continuous symmetry, we expect that the vestigial phase breaks the same point-group symmetry as the mean-field solution. From this line of reasoning we expect to find a vestigial xy LC phase [$\vec{l} = (l, l)$ without long-range PDW order] above the transition to the xy ME-PDW. Surprisingly, for $0.5 < \beta < 1$, $\beta < \alpha$, we find that the xy LC phase can become unstable to an $x^2 - y^2$ LC phase [$\vec{l} = (l, 0)$] at higher temperature (see Fig. 4). Thus, the mean-field ground state is preempted by a low-temperature vestigial phase, sharing the same xy symmetry, and a high-temperature vestigial phase, with a different symmetry ($x^2 - y^2$). This possibility can be understood as a result of a fluctuation-induced transition between the mean-field ground and first excited states, which are both listed in Table II. Near this transition we find a state with *soft* nematic order, which is discussed in Secs. IV C and V.

In the continuation of this section we derive the content of Table II and study the phase diagram for $0.5 < \beta < 1$, $\beta < \alpha$, presented in Fig. 4. Some details are left for Appendixes A, B, and C.

A. Note on primary and subleading nematic orders

Again, for simplicity, we assume that only sector A is stable for the following development. However, it is important to note that the A and B sectors support different *primary* nematic fields, $N_{x^2-y^2}$ and N_{xy}, respectively, while both support the *subleading* nematic order $l_x^2 - l_y^2$ and $l_x l_y$. A finite LC order implies subleading nematic order $l_x^2 - l_y^2$, $l_x l_y$ transforming as B_{1g} and B_{2g}, respectively. The subleading nematic orders are to fourth order in PDW fields, while the primary nematic fields $N_{x^2-y^2}$, N_{xy} (listed in Table I) are to second order

in the PDW fields. Specifically, sector A only supports the primary nematic order $N_{x^2-y^2}$, but not N_{xy}. Thus, an xy LC order, $\vec{l} = (l, l)$, implies subleading B_{2g} nematic order, $l_x l_y$, but no primary, N_{xy}. In contrast, an $x^2 - y^2$ LC order implies both secondary and primary B_{1g} order, $l_x^2 - l_y^2$, $N_{x^2-y^2}$. (The reverse is true for the B sector.)

B. Vestigial mean-field solutions

We will explore the possibility of vestigial ordering by considering the mean-field solutions for $\psi, N_{x^2-y^2}, \vec{l}$, of the effective action (17), given by the solutions to the mean-field equations $\frac{\partial S_{\text{eff}}}{\partial \Phi} = 0 \Rightarrow \frac{\delta S_{\text{eff}}}{\delta \psi} = 0, \frac{\delta S_{\text{eff}}}{\delta N_{x^2-y^2}} = 0, \frac{\delta S_{\text{eff}}}{\delta l_{x,y}} = 0$:

$$\psi = u_0 \int_{\vec{k}} \chi_{\mathbf{Q}_1}(\vec{k}) + \chi_{-\mathbf{Q}_1}(\vec{k}) + \chi_{\mathbf{Q}_2}(\vec{k}) + \chi_{-\mathbf{Q}_2}(\vec{k}),$$

$$N_{x^2-y^2} = u_1 \int_{\vec{k}} \chi_{\mathbf{Q}_1}(\vec{k}) + \chi_{-\mathbf{Q}_1}(\vec{k}) - \chi_{\mathbf{Q}_2}(\vec{k}) - \chi_{-\mathbf{Q}_2}(\vec{k}),$$

$$l_x = u_2 \int_{\vec{k}} \chi_{\mathbf{Q}_1}(\vec{k}) - \chi_{-\mathbf{Q}_1}(\vec{k}),$$

$$l_y = u_2 \int_{\vec{k}} \chi_{\mathbf{Q}_2}(\vec{k}) - \chi_{-\mathbf{Q}_2}(\vec{k}), \quad (23)$$

where

$$\chi_{\pm\mathbf{Q}_1}(\vec{k}) = \frac{1}{\chi'_x(\vec{k})^{-1} + N_{x^2-y^2} \pm l_x},$$

$$\chi_{\pm\mathbf{Q}_2}(\vec{k}) = \frac{1}{\chi'_y(\vec{k})^{-1} - N_{x^2-y^2} \pm l_y}, \quad (24)$$

are the static susceptibilities with $\chi'_{x,y}(\vec{k})^{-1} = r' + \kappa_1(k_x^2 + k_y^2) \pm \kappa_2(k_x^2 - k_y^2)$, $r' = r + \psi + \gamma_0|\Delta_0|^2$.

The most extreme example of a preemptive transition into a vestigial phase happens in two dimensions, where the integral for ψ is infrared divergent. This divergence leads to
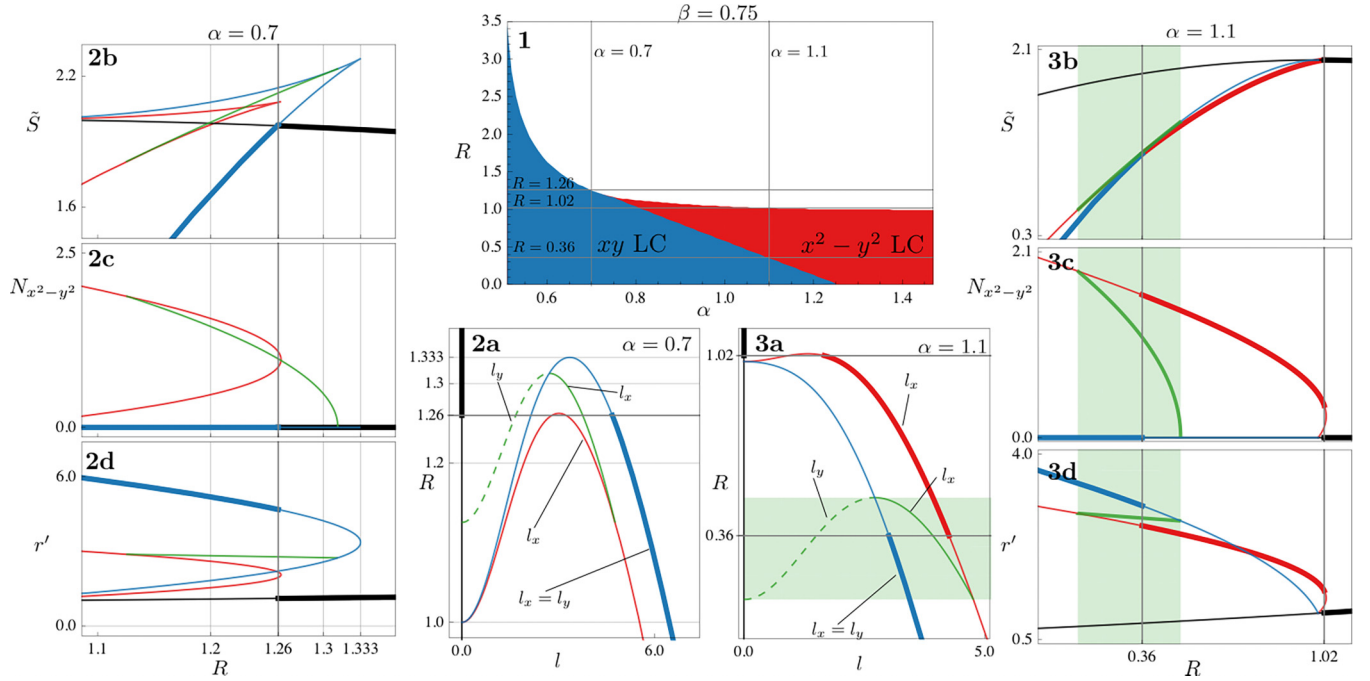
FIG. 4. Two solved systems for $\beta = 0.75$ with three metastable phases: Normal phase with no order (black lines), xy LC phase $l_x = l_y$ (blue) and $x^2 - y^2$ LC phase $l_x > 0$, $l_y = 0$ (red). (a) Phase diagram as a function of α and R ($R = 0$ is an arbitrary starting point). (b) Developing of order for $\alpha = 0.7$. Thick lines corresponds to the global stable phase [in (a)] while thin lines corresponds to local extrema of the action. Here xy LC is the only stable ordered phase, reached through a first order transition. The xy and $x^2 - y^2$ LC have two branches which develop as R is lowered (b1), one stable (large l) and one unstable, as can be seen from the energy relation (b2). The saddle-point solution (green) represents an unstable branch $l_x \neq l_y > 0$ that extrapolates between the xy and x^2y^2 LC phase. (b1) Solid (dashed) green represents l_x (l_y) connecting the $l_x = l_y$ solution with $l_x > 0$, $l_y = 0$. [(b3), (b4)] The development of the B_{1g} nematic order, $N_{x^2-y^2}$, and the renormalized static susceptibility r'. (c) Developing of order for $\alpha = 1.1$. Here, both xy and $x^2 - y^2$ LC are possible stable phases. At $R = 1.02$ the system goes through (c1) a first-order transition to a state with finite l, as well as (c3) finite nematic order. At $R = 0.36$ (c2) the xy and $x^2 - y^2$ LC becomes degenerate and (c1) another first-order transition to the xy LC phase occurs, where (c3) the *primary* B_{1g} nematic order is lost. (c2) The saddle-point solution again extrapolates between the $x^2 - y^2$ and xy LC states and near transition $R = 0.36$ all three states are near degenerate. (c4) The renormalized static susceptibility r'.

finite PDW susceptibilities (24), implying no long-range PDW order. This is just a restatement of the Mermin-Wagner theorem: Continuous symmetries will not form long-range order at finite temperature in two dimensions. The vestigial order parameters, however, being discrete Ising-like orders can break the point-group symmetries. Continuing with the 2D case, we find the mean-field equations of (17) as

$$r' = r^R - \frac{u_0}{4\pi\overline{\kappa}} \ln\left[(r' + N_{x^2-y^2})^2 - l_x^2\right]$$
$$\times \left[(r' - N_{x^2-y^2})^2 - l_y^2\right], \tag{25a}$$

$$N_{x^2-y^2} = -\frac{u_1}{4\pi\overline{\kappa}} \ln \frac{(r' + N_{x^2-y^2})^2 - l_x^2}{(r' - N_{x^2-y^2})^2 - l_y^2}, \tag{25b}$$

$$l_x = -\frac{u_2}{4\pi\overline{\kappa}} \ln \frac{r' + N_{x^2-y^2} + l_x}{r' + N_{x^2-y^2} - l_x}, \tag{25c}$$

$$l_y = -\frac{u_2}{4\pi\overline{\kappa}} \ln \frac{r' - N_{x^2-y^2} + l_y}{r' - N_{x^2-y^2} - l_y}, \tag{25d}$$

where we introduced $r^R = r + \frac{u_0}{\pi\overline{\kappa}} \ln(\overline{\kappa}\Lambda^2)$, $\overline{\kappa} = \sqrt{|\kappa_1^2 - \kappa_2^2|}$, and Λ as the momentum cutoff. Instead of using ψ we have expressed the mean-field equations in terms of $r' = r + \psi$,

where we assume $\Delta_0 = 0$. This is natural since ψ describes Gaussian fluctuations of the PDW fields, which renormalizes the bare static susceptibility r^{-1}.

Care must be taken when considering solutions to Eqs. (25). First, in the absence of long-range PDW order, only solutions fulfilling $r' + N_{x^2-y^2} \pm l_x$, $r' - N_{x^2-y^2} \pm l_y > 0$ can be considered physical. Second, solutions to Eqs. (25) are generally singular, meaning that solutions with finite order do not generally coincide with solutions without order in the limiting cases. Therefore, we will have to consider all possible combinations of ordering independently. In addition to the trivial normal state without any ordering we find the following solutions.

(i) xy LC state: LC ordered state with xy nematic order, $l_x = l_y \neq 0$ [69]. Solutions are presented in Appendix A.

(ii) LC saddle-point solution: Unstable LC ordered state with both $x^2 - y^2$ and xy nematic order, $l_x \neq l_y \neq 0$. Solutions are presented in Appendix A.

(iii) $x^2 - y^2$ LC state: LC ordered state with with $x^2 - y^2$ nematic order, $l_{x,y} \neq 0$, $l_{y,x} = 0$, and $N_{x^2-y^2} \neq 0$. Solutions are presented in Appendix B.

Solutions with only nematic order and no LC order are of secondary interest and presented in Appendix D, for completeness.
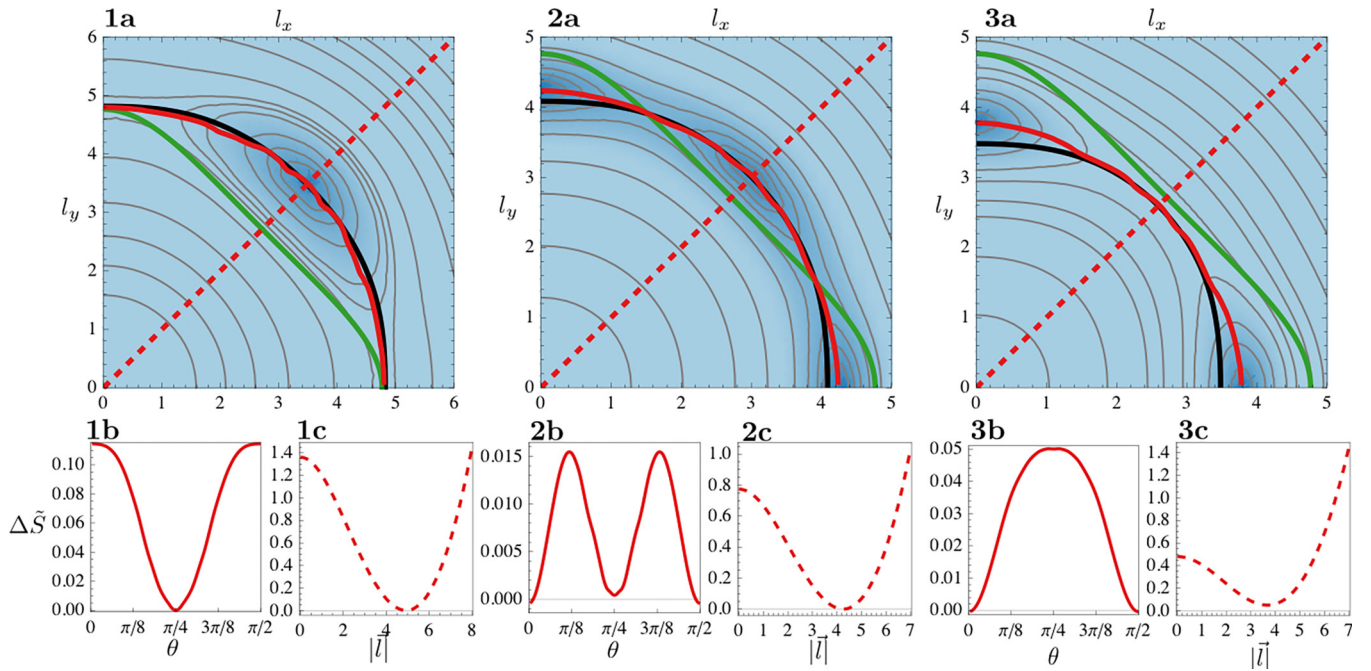
FIG. 5. Energy with respect to the ground state for arbitrary $\vec{l}$ from Eq. (C2) after solving for Eqs. (25a) and (25b) with $\beta = 0.75$, $\alpha = 1.1$, and $R = 0.10, 0.36, 0.55$. [(a), (d), (g)] Equipotential contours of energy in gray, with dark shading indicating low energy. Solutions to Eqs. (A2a) and (A2b) in black and green, respectively ($l_x = l_y$ solutions are removed from the latter). [(b), (c), (e), (f), (h), (i)] Energy along the valley (solid red line) and the radial direction (dashed red line). [(a)–(c)] $R = 0.10$, below the transition between the xy and $x^2 - y^2$ LC phase in Fig. 4. The green line does not cross the black line, thus there exists no intermediate extreme along the valley. $x^2 - y^2$, xy LC are unstable and stable respectively [see (b)]. (c) Energy in the radial direction. [(d)–(f)] Same as in (a)–(c) for $R = 0.36$ near the transition. (d) Intersection between the green and black curves, corresponding to intermediate extrema along the valley direction. (e) Both xy and $x^2 - y^2$ LC correspond to local minima. (f) Energy in the radial direction. [(g)–(i)] Same as in (d)–(f) for $R = 0.55$ above the transition where xy LC is stable and $x^2 - y^2$ LC unstable, as can be seen in (h).

In finding the vestigial mean-field solutions it is convenient to rescale the order parameters to unitless quantities, $\tilde{l}_x = 2\pi\bar{\kappa} l_x/|u_2|$, and equivalently for other variables. (See Appendixes A and B for details.) However, for notational clarity we will suppress the tilde even when the parameters should be interpreted as unitless. The susceptibility gains an additional shift

$$R = \tilde{r}^R - 2\alpha \ln\left(\frac{|u_2|}{2\pi\bar{\kappa}}\right). \tag{26}$$

Here R is assumed to be tunable with temperature through its dependence on the bare susceptibility r.

The mean-field solutions only guarantee local stability, and we must compare the absolute energy of the different phases in order to find the ground state. The energy is presented in Appendix C. The energy expression (C2) was used to find the stable vestigial phases listed in Table II. For $0 < \beta < 0.5$ ($1 < \beta$), the $x^2 - y^2$ (xy) LC state is the stable state, regardless of α (and for low enough R). In contrast, for $0.5 < \beta < 1$, there is a transition between the $x^2 - y^2$ and xy LC states for $\beta < \alpha$, as $R \propto T$) is lowered, while the xy LC state is the only possible ordered state for $\alpha < \beta$. Thus, after including fluctuations, there is an induced transition between the would-be mean-field ground and first excited states (see Table II), resulting in a high-temperature $x^2 - y^2$ LC phase and low-temperature xy LC phase, separated by a first-order transition.

C. Phase diagram and the $x^2 - y^2$ and xy LC transition

As a representative case of $0.5 < \beta < 1$, $\beta < \alpha$, the phase diagram and the evolution of the order parameters are presented in Fig. 4 for $\beta = 0.75$, $\alpha = 0.7$, and $\alpha = 1.1$. (For $\alpha = 0.75$ the normal, the xy and $x^2 - y^2$ LC phases all coexist. It is possible to show that this holds in general for $\alpha = \beta$.)

The saddle-point solution ($l_x \neq l_y > 0$) only has support for a finite range of $R \in (R_{\min}, R_{\max})$, as indicated by the green regions in Figs. 4(c1)–4(c4), and forms closed paths in the (l_x, l_y) plane [see also Fig. 7(a) in Appendix A]. As R is tuned from $R_{\max}$ to $R_{\min}$, by lowering the temperature, $\vec{l}$ twists from $l_x = l_y$ with $N_{x^2-y^2} = 0$ to $l_x > 0$, $l_y = 0$ with $N_{x^2-y^2} > 0$.

To explore this transition further we consider the absolute energy in terms of $\vec{l}$ [70]. The energy is presented in Fig. 5 for $\alpha = 1.1$, $\beta = 0.75$, just below ($R = 0.10$) and above ($R = 0.55$) the support for the saddle-point solution, as well as near the transition $R = 0.36$.

The xy and $x^2 - y^2$ LC solutions lie on a semicircular shaped valley in the energy landscape. Because of periodicity, the number of maxima equals the number of minima. Thus, in order for the xy and $x^2 - y^2$ LC to be simultaneously stable, two intermediate maxima have to be introduced along the valley (in each quadrant). These are the $l_x \neq l_y$ solutions, and their energy can be seen as the height of the barrier between the two (meta)stable solutions. Nevertheless, these are saddle-point solutions in the full energy landscape. As is seen

both from Figs. 4(c2) and 5(b2), this barrier height is small compared to the energy scale in the radial direction. Thus, the solutions are easily excited along the valley direction.

The relative smallness of the stiffness in the valley direction should be understood as a result of the valley direction being a compact dimension whose length is tunable to zero. Alternatively, it follows from expanding around a rotational invariant point $\vec{l} = 0$. This effect is perhaps most easily seen from comparing Figs. 5(a)–5(c) and 5(g)–5(i) with Figs. 5(d)–5(f). In the former, the dispersion is only about twice as soft in the valley direction, while in the latter, the inclusion of three additional stationary points forces the dispersion to become even flatter in the valley direction. In the limit $\vec{l} \to 0$, this feature is expected to become more pronounced. To confirm, we expand Eqs. (A2a) and (A2b) for small $\vec{l}$, and find

$$\frac{6(1-R)}{\alpha - 1} = l_x^2 + l_y^2 + \mathcal{O}(l^4),$$

$$\frac{30(1-\beta)}{\beta} = l_x^2 + l_y^2 + \mathcal{O}(l^4), \tag{27}$$

describing two concentric circles. This implies that at $R = \frac{5-4\beta}{\beta} + \frac{5(\beta-1)}{\beta}\alpha$ all points around the valley will be arbitrarily close to a local maximum; thus the valley direction will be essentially flat. This expansion becomes exact for $\beta \to 1^-$, and according to Table II, there will be a second-order phase transition for $\alpha > \beta$, where the xy and $x^2 - y^2$ LC states are degenerate. Thus, the first-order transition gets turned into a second-order transition. As a corollary, we expect a small stiffness in the valley direction whenever there is only a small region of support for the $x^2 - y^2$ solutions.

V. SOFT NEMATIC STATE

We have seen how the vicinity of the first-order transition between xy and $x^2 - y^2$ LC gives rise to an arbitrarily flat energy landscape, associated with a rotation of the LC order. Thus, a small field would be able to pin the LC order in any direction, promoting a state with, in general, both B$_{1g}$ and B$_{2g}$ nematic order. For concreteness, we can consider a correction to the superconducting mass, like the one found in Eqs. (18), due to the LC order

$$S = \begin{bmatrix} g_1(l_x^2 - l_y^2)/2 & g_2 l_x l_y \\ g_2 l_x l_y & -g_1(l_x^2 - l_y^2)/2 \end{bmatrix}. \tag{28}$$

The principal direction of S will in general not be aligned with the crystallographic axis, as well as being easily pinned in any direction. We will refer to this as a "soft" nematic state. (Note that S does not constitute an XY nematic order parameter unless $g_1 = g_2$.)

There is some evidence for such a soft nematic state for the cuprates. A detachment of the nematic director from the lattice is seen in transport measurements on LSCO films [61], a signature which is strongest near optimum doping. This state is also expected to be sensitive to quenched disorder, which might explain the decreasing nematic domain size in bismuth strontium calcium copper oxide (BSCCO) [8], approaching optimum doping. This would suggest that the underlying nematic state seen in both LSCO and BSCCO is of the same

origin, an underlying xy ME-PDW preempted by an xy and/or $x^2 - y^2$ LC state in turn setting up a soft nematic state, of the type described here; in LSCO the nematicity may be aligned by an external symmetry breaking field, while in BSCCO it is pinned to impurities. We include this scenario in the inset of Fig. 1, where the vestigial nematic phase is divided into a high- and low-temperature phases with $x^2 - y^2$ and xy nematic order, respectively, with a soft nematic state at the boundary of the two phases.

Emergent overdamped Goldstone mode

The approximate rotational symmetry for the LC order near the first-order transition implies the existence of low-lying collective excitations. In the limit of an exact rotational symmetry this would correspond to a Goldstone mode. To explore the signatures of the soft nematic state near the transition we here consider the the spectral function of this "emergent" Goldstone mode.

The collective modes of the xy and $x^2 - y^2$ LC states involve not only the LC order but couple all fields in the complete $\psi, N_{x^2-y^2}, \vec{l}$ space; as $\vec{l}$ change, $N_{x^2-y^2}$ and ψ change accordingly. Thus, in general, a collective mode is associated with variations in the combined space of $\Phi = [\psi, N_{x^2-y^2}, l_x, l_y]$. In Eq. (7), we neglected the time dependence of the (bosonic) fields, corresponding to a high-temperature (classical) limit, where only the first bosonic Matsubara frequency is kept. Now we reintroduce the Matsubara frequencies to find the excitation spectra by analytic continuation to real frequencies.

The PDW part of the effective action (7) (for the A sector) can be written as

$$S_{\text{eff}}(\{\Delta_{\mathbf{Q}}\}, \psi, N_{x^2-y^2}, \vec{l})$$

$$= -\frac{1}{T} \int_\mu \frac{|\psi_\mu|^2}{2u_0} + \frac{|N_{x^2-y^2,\mu}|^2}{2u_1} + \frac{|\vec{l}_\mu|^2}{2u_2} + \int_{\mu,\mu'} \vec{\Delta}_\mu^\dagger \overline{\mathcal{G}}_{\mu;\mu'}^{-1} \vec{\Delta}_{\mu'}, \tag{29}$$

where we included an integral $T \int_0^{1/T} d\tau$ and fields in the Matsubara representation $f(i\omega_n) = \int_0^{1/T} d\tau\, e^{-i\omega_n \tau} f(\tau)$, with the bosonic Matsubara frequencies $\omega_n = 2\pi n T$. We introduced the short-hand notation $\mu = i\omega, \vec{k}$ and $\vec{\Delta} = [\Delta_{\mathbf{Q}_1} \Delta_{-\mathbf{Q}_1} \Delta_{\mathbf{Q}_2} \Delta_{-\mathbf{Q}_2}]$, $\int_\tau = \int_0^{1/T} d\tau$ and $\int_\mu = T \sum_{i\omega_n} \int_{\vec{q}}$. We find the kernel $\mathcal{G}$ as

$$\mathcal{G}_{11,\mu;\mu'}^{-1} = (-i\omega + T\chi_x^{-1}(\vec{k}))\delta_{\mu,\mu'}$$
$$+ \psi_{\mu-\mu'} + N_{x^2-y^2,\mu-\mu'} + l_{x,\mu-\mu'},$$

$$\mathcal{G}_{22,\mu;\mu'}^{-1} = (-i\omega + T\chi_x^{-1}(\vec{k}))\delta_{\mu,\mu'}$$
$$+ \psi_{\mu-\mu'} + N_{x^2-y^2,\mu-\mu'} - l_{x,\mu-\mu'},$$

$$\mathcal{G}_{33,\mu;\mu'}^{-1} = (-i\omega + T\chi_y^{-1}(\vec{k}))\delta_{\mu,\mu'}$$
$$+ \psi_{\mu-\mu'} - N_{x^2-y^2,\mu-\mu'} + l_{y,\mu-\mu'},$$

$$\mathcal{G}_{44,\mu;\mu'}^{-1} = (-i\omega + T\chi_y^{-1}(\vec{k}))\delta_{\mu,\mu'}$$
$$+ \psi_{\mu-\mu'} - N_{x^2-y^2,\mu-\mu'} - l_{y,\mu-\mu'}, \tag{30}$$

where $\chi_{x,y}^{-1} = r + \kappa_1(k_x^2 + k_y^2) \pm \kappa_2(k_x^2 - k_y^2)$, and $\delta_{\mu,\mu'} = \delta(\vec{k} - \vec{k}')\delta_{i\omega,i\omega'}/T$. We assume that the PDW fields are

coherently propagating, and not damped. (This would be the case if PDW arose from a strong-coupled BEC scenario [56].) The effective action is found in terms of Φ by integrating over the PDW fields. We proceed by expanding around the uniform mean-field solution $\frac{\delta S_{\text{eff}}}{\delta \Phi} = 0$, given by Φ_0,

$$\Phi(i\nu_n, \vec{q}) = \Phi_0 \delta_{n,0} \delta(\vec{q}) + \delta\Phi(i\nu_n, \vec{q}). \tag{31}$$

Expanding the action to second order in $\delta\Phi$

$$S_{\text{eff}}(\psi, N_{x^2-y^2}, \vec{l}) \approx S_{\text{eff}}^{(0)}(\psi_0, N_{x^2-y^2,0}, \vec{l}_0) + S_{\text{eff}}^{(2)}(\psi, N_{x^2-y^2}, \vec{l}). \tag{32}$$

In the high-temperature limit, keeping only the first Matsubara term $n = 0$, $S_{\text{eff}}^{(0)}(\psi, N_{x^2-y^2}, \vec{l})$ is given by Eq. (14) (with Δ_0 reinserted). The correction can be written

$$S_{\text{eff}}^{(2)} = \int_{\mu} \frac{1}{2} \delta\Phi_i(\mu) \mathcal{L}_{ij}^{-1}(\mu) \delta\Phi_j(\mu),$$

$$\mathcal{L}_{ij}^{-1}(i\nu_n, \vec{q}) = \frac{-\delta_{ij}}{Tu_i} - \overline{\Sigma}_{ij}(i\nu_n, \vec{q}). \tag{33}$$

Here $\mathcal{L}$ is the propagator of fluctuations of Φ, with $u_i = [u_0, u_1, u_2, u_2]$. The self-energy term is given by

$$\overline{\Sigma} = \begin{pmatrix} \Sigma_1 + \Sigma_2 + \Sigma_3 + \Sigma_4 & \Sigma_1 + \Sigma_2 - \Sigma_3 - \Sigma_4 & \Sigma_1 - \Sigma_2 & \Sigma_3 - \Sigma_4 \\ \Sigma_1 + \Sigma_2 - \Sigma_3 - \Sigma_4 & \Sigma_1 + \Sigma_2 + \Sigma_3 + \Sigma_4 & \Sigma_1 - \Sigma_2 & \Sigma_4 - \Sigma_3 \\ \Sigma_1 - \Sigma_2 & \Sigma_1 - \Sigma_2 & \Sigma_1 + \Sigma_2 & 0 \\ \Sigma_3 - \Sigma_4 & \Sigma_4 - \Sigma_3 & 0 & \Sigma_3 + \Sigma_4 \end{pmatrix}, \tag{34}$$

where

$$\Sigma_i(i\nu_n, \vec{q}) = \int_{i\omega, \vec{k}} G_i(i\omega + i\nu, \vec{k} + \vec{q}) G_i(i\omega, \vec{k}), \tag{35}$$

and $G_i^{-1}(i\omega, \vec{k}) = -i\omega + T\chi_{\mathbf{Q}(i)}^{-1}(\vec{k})$ where $\mathbf{Q}(i) = [\mathbf{Q}_1, -\mathbf{Q}_1, \mathbf{Q}_2, -\mathbf{Q}_2]$. The propagator $\mathcal{L}_{ij}(i\nu_n, \vec{q})$ is in general off-diagonal. However, when approaching the $x^2 - y^2$ to xy LC transition from the x^2-y^2 LC state, with $l_x = l_0$, $l_y = 0$ and $N_{x^2-y^2} \neq 0$, $\overline{\Sigma}_{ij}(i\nu_n, \vec{q})$ is block diagonal, $\overline{\Sigma}_{ij} = \overline{\Sigma}_{ab} \oplus \overline{\Sigma}_{44}$, $a, b = 1, 2, 3$. In this case the valley direction lies solely along l_y, with all other fields stationary.

The static, zero-frequency part of the propagator $\mathcal{L}_{ij}^{-1}(0, 0)$ is associated with the stiffness to uniform deformation. Here $\mathcal{L}_{44}^{-1}(0, 0)$ can be related with the stiffness along the valley direction, which we set to zero and identify it with the transverse propagator for a nematic director along the x axis, $\mathcal{L}_{44}^{-1} = \mathcal{L}_{\perp,x}^{-1}$. After analytic continuation of

$$\overline{\Sigma}_{44}(i\nu_n, \vec{q}) = 2 \int_{i\omega, \vec{k}} G_4(i\omega_n + i\nu_n, \vec{k} + \vec{q}) G_4(i\omega_n, \vec{k}), \tag{36}$$

we can obtain the retarded transverse propagator. In the high-temperature limit, after expanding in $\vec{q}$ and ν/q (assuming $r \gg N_{x^2-y^2}, \vec{l}$, i.e., far from the PDW transition) we find

$$\mathcal{L}_{\perp,x}^{-1}(\nu, \vec{q}) = \eta \tilde{q}^2 - i\eta' s + \mathcal{O}(s\tilde{q}) + \mathcal{O}(s^3), \tag{37}$$

where $s = \nu/\tilde{q}$, $\eta = \frac{1}{12\pi T \bar{\kappa}} \frac{1}{r^2}$, $\eta' = \frac{1}{8T^2 \bar{\kappa}} \frac{1}{r^{3/2}}$, and $\tilde{q} = q\sqrt{\kappa_1 - \kappa_2 \cos(2\varphi)}$, where φ is the angle of $\vec{q}$ to the x axis. In Fig. 6, the spectral density $\text{Im}(\mathcal{L}_\perp)$ is shown, and we see an overdamped bosonic mode, with $\nu \propto iq^3$.

These results are reminiscent of the results for a nematic Fermi fluid [71], where an overdamped Goldstone mode is
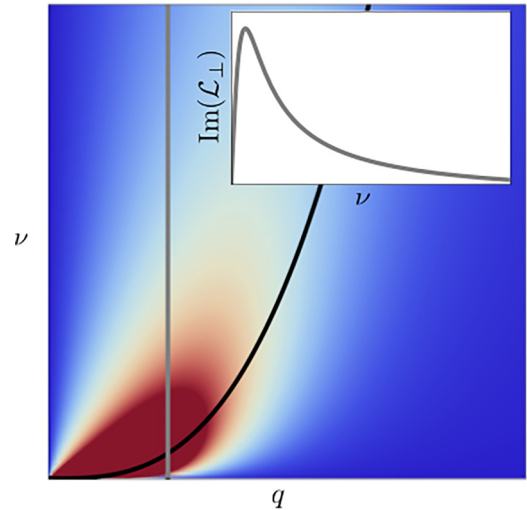

FIG. 6. Spectral density of the Goldstone mode at the enhanced symmetry point $\text{Im}(\mathcal{L}_\perp(\nu, \vec{q}))$. The black line shows the peak of the spectral density at fixed $\vec{q}$. The inset shows the frequency dependence of the spectral density along the gray line.

found within the broken symmetry phase. (The reason has to do with the noncommuting property of the broken symmetry and translation [72].) In a fermionic system, an overdamped bosonic mode coupling to the fermions usually leads to the destruction of the Fermi liquid. This is of special interest in cuprates as a possible origin of the strange metal phase [6,73].

A Goldstone mode associated with spatial rotation is not expected in a crystalline system since there is no rotational symmetry. However, as seen in this work, a competition between a vestigial xy and an x^2-y^2 LC phase leads to a very small gap and an emerging symmetry. It is intriguing to note that this phenomenology again points towards an emergent rotational symmetry near the overdoped critical point (possibly a soft nematic state), over which the strange metal phase is located. Indeed, at this level, these results are only speculative. First of all, in the model considered here, the bosonic mode does not couple directly to fermions, but to PDW fluctuations. The fate of the PDW fields and the underlying fermions is left for future work.

VI. SUMMARY AND OUTLOOK

In this paper, we study vestigial orders of a PDW state with pair momenta that are aligned with the high-symmetry directions of a tetragonal crystal, focusing on phases that only break the point-group symmetry. Of particular interest is the influence of vestigial nematic order on a homogenous single-component superconductor, giving rise to an anisotropic superfluid stiffness. We stress that if the nematicity arises from a PDW state, i.e., from finite momentum fluctuations of the superconducting field itself, the superconductor can become highly susceptible to this nematic distortion due to the natural proximity of a Lifshitz point with vanishing superfluid stiffness. Crucially, even a nominally weak nematic field, as observed through anisotropy of the normal electron response or the superconducting gap, may give a large relative renormalization of a small stiffness. We argue that this may explain

why the observed anisotropy in transport measurements on LSCO [61] can be ascribed to highly anisotropic superconducting fluctuations coexisting with an essentially isotropic normal conductivity [58]. Probing vortex dynamics, also expected to be sensitive to stiffness anisotropy, near T_c, could be a fruitful pursuit to investigate this unusual manifestation of nematicity further.

In the later part of the paper we focus on vestigial orders of a magnetoelectric (ME) PDW, containing both nematic order and loop-current-type order. We have shown that a preemptive transition into a vestigial phase of an ME-PDW with B_{1g} ($x^2 - y^2$) nematic order can split into high- and low-temperature phases, that correspond to distinct B_{1g} and B_{2g} (xy) phases. This feature is not specific to PDW, but is expected for any other field transforming in the $A_{1g} \oplus B_{1g} \oplus E_u$ (or $A_{1g} \oplus B_{2g} \oplus E_u$) representation. Near the transition between the high- and low-temperature phases, the nematic order will be soft and easy to pin in either direction, yielding an approximate rotational symmetry, with possible relevance to observations of nematic order in LSCO and BSCCO. Also, as a start for further investigation, the emergence of an overdamped Goldstone mode due to this approximate rotational symmetry may have interesting implications for the single-particle properties of electrons coupling to this mode.

In conclusion, the results lend support and warrant further investigation into the proposal of pair-density wave order as the underlying source of the abundance of broken symmetries and exotic phenomenology seen in the cuprate superconductors.

Note added. Recently, an experimental study of overdoped $Bi_2Sr_2CaCu_2O_{8+x}$ using scanning Josephson tunneling microscopy has presented evidence for a nematic state with short-range PDW order, interpreted as a disorder-pinned realization of a state with vestigial nematic PDW order [74].

APPENDIX A: *xy* LC STATE AND SADDLE-POINT SOLUTION, $l_x, l_y \neq 0$

Let us start by assuming that both l_x and l_y are nonzero. All Eqs. (25) respect the symmetry $l_{x,y} \to -l_{x,y}$, and thus we can focus on $l_{x,y} > 0$. Nontrivial $l_x, l_y > 0$ solutions of Eqs. (25c) and (25d) take the form

$$r' \pm N_{x^2-y^2} = -l_{x,y} \coth\left(\frac{2\pi\bar{\kappa}}{u_2}l_{x,y}\right), \qquad \text{(A1)}$$

from which we see the need for $u_2 < 0$ to ensure $r' \pm N_{x^2-y^2} - l_{x,y} > 0$. The existence of primary B_{1g} nematic order, $N_{x^2-y^2} \neq 0$, is equivalent to $l_x \neq l_y$ as seen from Eq. (25b) which ensures $N_{x^2-y^2} \neq 0$ if $l_x \neq l_y$, while Eqs. (25c) and (25d) imply $N_{x^2-y^2} = 0$ if $l_x = l_y$, unless $l_x = l_y = 0$. Only considering the A sector we do not find any primary (N_{xy}) B_{2g} nematic order for the $l_x = l_y$ solution. However, if both the A and B sectors were stable, the subleading ($l_x l_y$) B_{2g} nematic order would induce a finite primary B_{2g} nematic order N_{xy} (supported by sector B) through the coupling set by v_1 in Eq. (4). In Appendix E
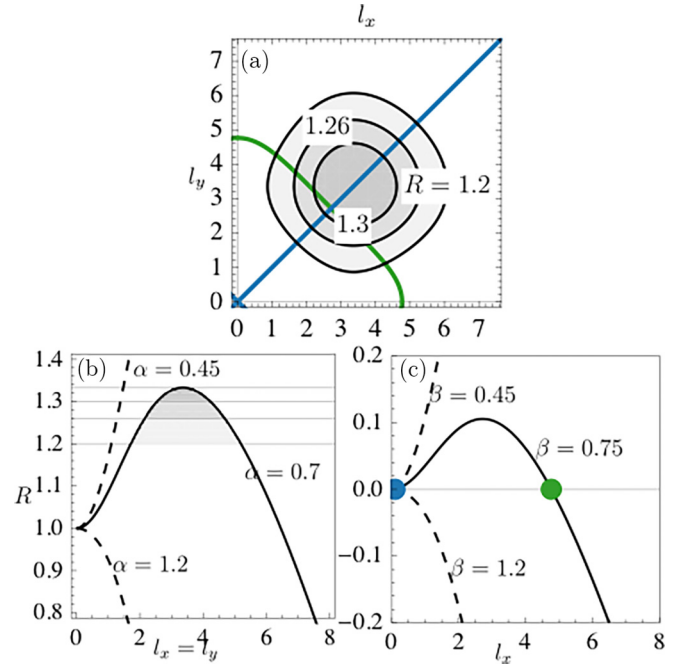

FIG. 7. (a) Solutions of Eqs. (A2) in the l_x, l_y plane. The black curves are solutions to Eq. (A2a), $\alpha = 0.7$ for $R = 1.2$, 1.26, 1.3, 1.33 (peak R). The blue line corresponds to the xy LC $l_x = l_y$ solutions to Eq. (A2b) for $\beta = 0.75$, while the saddle-point solution, $l_x \neq l_y$, is shown in green. Simultaneous solutions to Eqs. (A2) are given by the intersection of the blue (or green) line with the black line. (b) Right-hand side of Eq. (A2a) for $\alpha = 0.45$, 0.7, 1.2 along the $\vec{l}$ diagonal $l_x = l_y$, for which Eq. (A2b) is trivially fulfilled. For $\alpha < 0.5$ unstable solutions exist for $R > 1$. For $\alpha > 1$ there are stable solutions for $R < 1$. When $0.5 < \alpha < 1$ solutions occur for a finite l, corresponding to a first-order transition. (c) Right-hand side of Eq. (A2b) for $\beta = 0.45$, 0.75, 1.2 plotted along the axial direction, $l_x > 0$, $l_y = 0$, as the condition is trivially zero for $l_x = l_y$. The blue dot indicates the intersection with the trivial zero solutions [blue lines in (a)], while the green dot indicates $l_x \neq l_y$ solutions [green lines in (a)]. $l_x \neq l_y$ solutions only exist for $0.5 < \beta < 1$.

we discuss the inclusion of both sectors, but for the present discussion this will be implicit.

Back to solving Eqs. (25): Using Eq. (A1) to simplify Eqs. (25a) and (25b) we receive two new (reduced) mean-field equations,

$$R = \frac{\tilde{l}_x \coth(\tilde{l}_x) + \tilde{l}_y \coth(\tilde{l}_y)}{2} + \alpha \ln\left(\frac{\tilde{l}_x \tilde{l}_y}{\sinh(\tilde{l}_x) \sinh(\tilde{l}_y)}\right), \qquad \text{(A2a)}$$

$$0 = \frac{\tilde{l}_x \coth(\tilde{l}_x) - \tilde{l}_y \coth(\tilde{l}_y)}{2} + \beta \ln\left(\frac{\tilde{l}_x \sinh(\tilde{l}_y)}{\tilde{l}_y \sinh(\tilde{l}_x)}\right), \qquad \text{(A2b)}$$

where we introduced the normalization $\tilde{l}_{x,y} = \frac{2\pi\bar{\kappa}l_{x,y}}{|u_2|}$, and $R = \tilde{r}^R - 2\alpha \ln(\frac{|u_2|}{2\pi\bar{\kappa}})$. Note that Eq. (A1) is not valid in the limit $l_{x,y} \to 0$, since it implies $r' \pm N_{x^2-y^2} = -\frac{u_2}{2\pi\bar{\kappa}}$, whereas Eqs. (25c) and (25d) do not put any constraints on $r' \pm N_{x^2-y^2}$. Thus $l_{x,y} = 0$ must be considered independently.

We find l_x and l_y by simultaneously solving Eqs. (A2a) and (A2b), which we can interpret graphically as in Fig. 7. Equation (A2b) is always solved for $l_x = l_y$, $N_{x^2-y^2} = 0$, cor-

responding to (meta)stable xy solutions. Equation (A2a) determines the evolution of $\vec{l}$, as R is changed. For $\alpha > 1$ there is an onset of stable solutions at $R = 1$ and $\vec{l} = 0$, corresponding to a second-order phase transition. For $0.5 < \alpha < 1$ a locally stable solution occurs at a finite $\vec{l}$ for some $R > 1$, implying a first-order phase transition.

Equation (A2b) also admits solutions with $l_x \neq l_y$, $N_{x^2-y^2} \neq 0$ for $0.5 < \beta < 1$, as can be seen from Fig. 7. These solutions, only supported for a finite range in R, will evolve along a curved path in the l_x, l_y plane, with a corresponding change in $N_{x^2-y^2}$ as R changes. These solutions are unstable; however, as will be clarified, their existence indicates that an xy and an $x^2 - y^2$ LC state are simultaneously stable. We will refer to this solution as the saddle-point solution since it constitutes a saddle point in the energy landscape. Indeed, in Sec. IV C we will see how $0.5 < \beta < 1$ admits a first-order transition between the xy and $x^2 - y^2$ LC states, with the possibility of a superheated and supercooled phase.

APPENDIX B: $x^2 - y^2$ LC STATE, $l_{x,y} \neq 0$, $l_{y,x} = 0$

Now we assume the stability of the $x^2 - y^2$ LC solutions with only one finite LC order component, say, $l_x > 0$. Equation (25d) puts no constraint on $r' - N_{x^2-y^2}$, while Eq. (25c) still implies $r' + N_{x^2-y^2} = -l_x \coth(\frac{2\pi\bar{\kappa}}{u_2} l_x)$. For physical solutions we must require $u_2 < 0$ as well as $r' - N_{x^2-y^2} > 0$. In this case, we can directly solve for r' and $N_{x^2-y^2}$ using Eqs. (25a) and (25b):

$$R = 2\alpha \ln \left(\frac{\tilde{l}_x}{\sinh(\tilde{l}_x)} \right) + \tilde{l}_x \coth(\tilde{l}_x) + (\alpha/\beta - 1)\tilde{N}_{x^2-y^2},$$
(B1a)

$$\tilde{N}_{x^2-y^2} = \frac{\tilde{l}_x}{2} \coth(\tilde{l}_x) - \beta W \left(\frac{\tilde{l}_x}{2\beta} \frac{\exp \left[\frac{\tilde{l}_x}{2\beta} \coth(\tilde{l}_x) \right]}{\sinh(\tilde{l}_x)} \right),$$
(B1b)

where $W(x)$ denotes the product logarithm. (For $l_y \neq 0$, $l_x = 0$, take $l_x \to l_y$ and $N_{x^2-y^2} \to -N_{x^2-y^2}$.) With $R \propto T$, nontrivial solutions evolve as R is lowered and Eq. (B1a) starts admitting solutions. For $\beta > 0.5$ and $\alpha > \frac{2+\beta}{4\beta-1}$ there is an onset of solutions at $R = 1$, $l_x = 0$, corresponding to a second-order phase transition. For $0.5 < \alpha < \frac{2+\beta}{4\beta-1}$, solutions occur at a finite l_x, corresponding to a first-order phase transition. With similar arguments for $\beta < 0.5$, we find the transitions included in Table II.

APPENDIX C: VESTIGIAL MEAN-FIELD ENERGY

The mean-field solutions only guarantee local stability, and we must compare the absolute energy of the different phases in order to find the ground state. Therefore, we need the normal-state solutions $N_{x^2-y^2} = 0$, $l_{x,y} = 0$, as well, which are always admitted by Eqs. (25b), (25c), and (25d). Equation (25a) is readily solved by

$$\tilde{r}' = 2\alpha W \left(\frac{e^{\frac{R}{2\alpha}}}{2\alpha} \right),$$
(C1)

requiring $r' > 0$.

The energy (17) has an explicit dependence on the cutoff Λ, which also renormalizes r. In the limit $\Lambda \to \infty$ the cutoff dependency can be absorbed in a constant energy term, given that the mean-field solution (25a) fulfills

$$\tilde{S} = \frac{\vec{\tilde{l}}^2}{2} - \frac{\tilde{l}_x}{2} \ln \frac{\tilde{r}' + \tilde{N}_{x^2-y^2} + \tilde{l}_x}{\tilde{r}' + \tilde{N}_{x^2-y^2} - \tilde{l}_x} - \frac{\tilde{l}_y}{2} \ln \frac{\tilde{r}' - \tilde{N}_{x^2-y^2} + \tilde{l}_y}{\tilde{r}' - \tilde{N}_{x^2-y^2} - \tilde{l}_y}$$
$$- \frac{\alpha}{8} \ln^2 \left((\tilde{r}' + \tilde{N}_{x^2-y^2})^2 - \tilde{l}_x^2 \right) \left((\tilde{r}' - \tilde{N}_{x^2-y^2})^2 - \tilde{l}_y^2 \right) + 2\tilde{r}'$$
$$- \frac{\tilde{r}'}{2} \ln \left((\tilde{r}' + \tilde{N}_{x^2-y^2})^2 - \tilde{l}_x^2 \right) \left((\tilde{r}' - \tilde{N}_{x^2-y^2})^2 - \tilde{l}_y^2 \right)$$
$$- \frac{\tilde{N}_{x^2-y^2}^2}{2\beta} - \frac{\tilde{N}_{x^2-y^2}}{2} \ln \left(\frac{(\tilde{r}' + \tilde{N}_{x^2-y^2})^2 - \tilde{l}_x^2}{(\tilde{r}' - \tilde{N}_{x^2-y^2})^2 - \tilde{l}_y^2} \right) + \text{const},$$
(C2)

where $\tilde{S} = \frac{S_0}{A} \frac{4\pi^2\bar{\kappa}^2}{|u_2|}$. This energy was used to find the stable vestigial phases listed in Table II.

It is important to note that the energy in Eq. (C2) only holds if Eq. (25a) is fulfilled. In order to present the energy as a function solely on $\vec{l}$, as in Fig. 5, we numerically solve Eqs. (25a) and (25b) given an arbitrary $\vec{l}$ by rewriting Eqs. (25a) and (25b) as first-order differential equations. As boundary conditions, Eq. (C1) and $N_{x^2-y^2} = 0$ were used at $\vec{l} = 0$. The absolute energy in terms of $\vec{l}$ was then found by inserting the solutions into Eq. (C2).

APPENDIX D: ADDITIONAL SOLUTIONS TO THE VESTIGIAL MEAN-FIELD EQUATIONS

One set of solutions that was not considered in the main development is that of only primary nematic order without LC order $N_{x^2-y^2} \neq 0$, $l_{x,y} = 0$, the pure nematic phase. Equations (25c) and (25d) always admit the $l_{x,y} = 0$ solution, and put no constraint on $N_{x^2-y^2}$ and r'. Nontrivial $N_{x^2-y^2} \neq 0$ solutions to Eq. (25b) take the form

$$r' = -N_{x^2-y^2} \coth \left(\frac{\pi\bar{\kappa}}{u_1} N_{x^2-y^2} \right),$$
(D1)

from which we find the expected requirement that we need $u_1 < 0$, in order for $r' \pm N_{x^2-y^2} > 0$. Assuming $u_1 <$ we can rewrite Eq. (D1) as

$$\hat{r}' = \hat{N}_{x^2-y^2} \coth(\hat{N}_{x^2-y^2}),$$
(D2)

which inserted into Eq. (25a) yields

$$\hat{R} = \hat{N}_{x^2-y^2} \coth(\hat{N}_{x^2-y^2}) + \frac{\alpha}{|\beta|} \ln \left(\frac{\hat{N}_{x^2-y^2}}{\sinh(\hat{N}_{x^2-y^2})} \right),$$
(D3)

where $\hat{N}_{x^2-y^2} = \frac{\pi\bar{\kappa}N_{x^2-y^2}}{|u_1|} = \frac{\tilde{N}_{x^2-y^2}}{2|\beta|}$ and $\hat{R} = \frac{R}{2|\beta|} - \frac{\alpha}{|\beta|} \ln(2|\beta|)$. Equation (D3) admits similar solutions as the xy LC case (A2a) (see Fig. 8), where we introduced $\delta = \frac{\alpha}{|\beta|} = \frac{u_0}{|u_1|}$. For $\delta < 1$ there is one unstable branch for $\hat{R} > 1$ and none for $\hat{R} < 1$. For $1 < \delta < 2$ there is an unstable branch for small $\hat{N}_{x^2-y^2}$ and a stable one for bigger $\hat{N}_{x^2-y^2}$, which leads to a first-order transition. For $\delta > 2$ there is one stable branch for $\hat{R} < 1$ and $\hat{N}_{x^2-y^2}$ evolves continuously from zero, yielding a second-order transition.
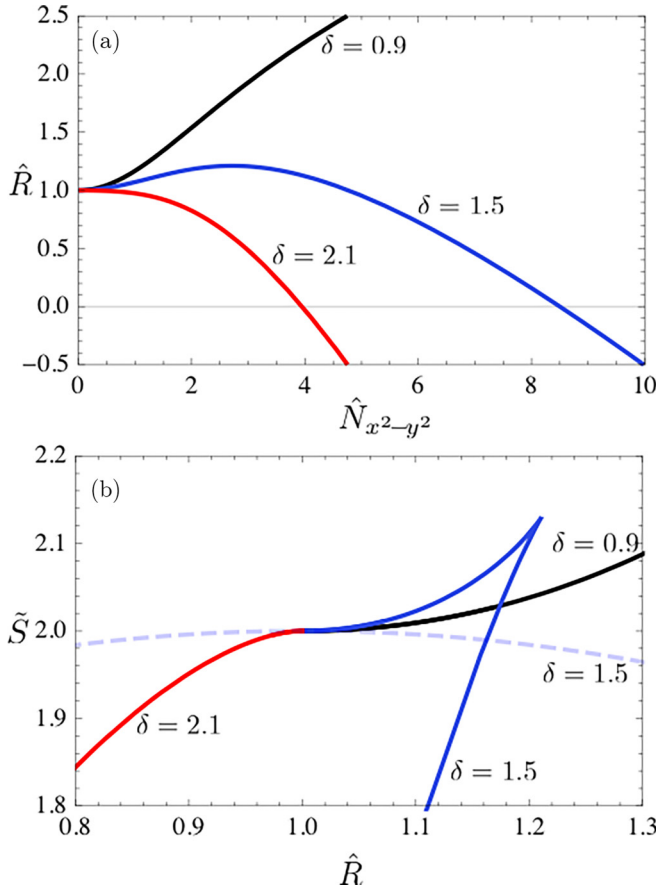
FIG. 8. Evolution of the pure nematic phase for a range of $\delta = \alpha/|\beta|$. The local stability of the pure nematic phase is only dependent on the parameter δ while the absolute value of β renormalizes the effective values of R, $N_{x^2-y^2}$, and S, thus affecting the relative stability compared to other phases. Here we used $\beta = -0.5$ for which $\hat{R} = R$, $\hat{N}_{x^2-y^2} = \tilde{N}_{x^2-y^2}$. (a) Equation (D3) plotted for a range of δ. For $\delta < 1$ there is no stable solution while for $\delta > 2$ stable solutions occur for $R < 1$ and the transition is second order. For $1 < \delta < 2$ there is one stable and one unstable branch and the transition will be first order.

So far u_2 has not entered the analysis and the $N_{x^2-y^2} \neq 0$, $l_{x,y} = 0$ solution is locally stable as long as $u_1 < 0$, regardless of u_2. For $u_2 > 0$ the pure nematic phase is the only locally stable solution. For $u_2 < 0$, the xy and x^2-y^2 LC phases are in general stable as well and we have to compare the absolute energy (C2) of the different phases. Taking into account the general stability of Eq. (4), $\alpha > 1 - \beta$ for $\beta < 0.5$, we find that the pure nematic phase is stable for $\beta < -0.5$ and the xy LC phase is stable for $-0.5 < \beta < 0$.

APPENDIX E: COUPLING BETWEEN A AND B SECTORS

Bilinears of our model transform in two distinct sectors, which we denote A and B. The stabilities of these two sectors, determined by the local minima of the dispersion (2), are independent, and we can consider situations where either one or both of the sectors are present.

The structures of both sectors are identical, and the above analysis holds equally for both sectors if we take into account that the states refer to the principal axes of the A and B sector

frames, respectively, which are rotated 45° to each other. For concreteness, the $x^2 - y^2$ LC and xy LC phase of the A sector map to the $\bar{x}^2 - \bar{y}^2 = xy$ LC and $\overline{xy} = x^2 - y^2$ LC phase of the B sector.

If both sectors are present they will couple through fourth-order terms, tuned by $v_{0,1}$ in Eq. (4). We will study this situation by including a weak interaction between the two sectors. Including nonzero couplings $v_{0,1}$ in Eq. (4) means that the matrix M in the Hubbard-Stratonovich transformation (5) will no longer be diagonal. Instead it will take the form

$$M = \begin{bmatrix} M_A & M_{AB} \\ M_{AB}^T & M_B \end{bmatrix}, \quad M_{AB} = \begin{bmatrix} v_0 & 0 & 0 & 0 \\ 0 & 0 & 0 & 0 \\ 0 & 0 & \frac{v_1}{\sqrt{2}} & -\frac{v_1}{\sqrt{2}} \\ 0 & 0 & \frac{v_1}{\sqrt{2}} & \frac{v_1}{\sqrt{2}} \end{bmatrix},$$

(E1)

and the auxiliary field vector $\Psi = [\psi_A, N_{x^2-y^2}, l_{A,x}, l_{A,y}, \psi, N_{xy}, l_{B,\bar{x}}, l_{B,\bar{y}}]$. Here $l_{B,\bar{x}}, l_{B,\bar{y}} = \frac{l_{B,x}+l_{B,y}}{\sqrt{2}}, \frac{l_{B,y}-l_{B,x}}{\sqrt{2}}$ are the B components along the (xy) diagonals. After integrating out the PDW field the effective action is given by (neglecting the superconducting field, which can be analogously introduced as before)

$$S_{\text{eff}}(\psi_A, N_{x^2-y^2}, \vec{l}_A, \psi_B, N_{xy}, \vec{l}_B)$$

$$= S_{\text{eff},\tilde{A}}(\psi_A, N_{x^2-y^2}, \vec{l}_A) + S_{\text{eff},\tilde{B}}(\psi_B, N_{xy}, \vec{l}_B)$$

$$- \left(\frac{\psi_A \psi_B}{\tilde{v}_0} + \frac{\vec{l}_A \cdot \vec{l}_B}{\tilde{v}_1} \right).$$

(E2)

The third term represents interaction between the A and B sectors, and the first two terms refer to the action of the A and B sectors, respectively [Eq. (17)]. Due to the inversion of the off-diagonal matrix, M, the couplings become renormalized [indicated by the tilde in (E2)]: $\tilde{u}_{0,(AB)} = u_{0,(AB)} - \frac{v_0^2}{u_{0,(AB)}}$, $\tilde{u}_{2,(AB)} = u_{2,(AB)} - \frac{v_1^2}{u_{2,(AB)}}$, $\tilde{v}_0 = v_0 - \frac{u_{0,A}u_{0,B}}{v_0}$, and $\tilde{v}_1 = v_1 - \frac{u_{2,A}u_{2,B}}{v_1}$. The two sectors do not couple directly through the primary nematic order parameters $N_{x^2-y^2}$, N_{xy}. The bilinear term in the LC orders of the two sectors implies mutual induction: A finite LC order in one sector will induce LC order in the other sector. This is evident from the (new) mean-field equations

$$\psi_A = \psi_B \frac{v_0}{u_{0,B}} + \frac{\tilde{u}_{0,A}}{\pi \overline{\kappa}_A} \ln \left(\overline{\kappa}_A \Lambda_A^2 \right)$$

$$- \frac{\tilde{u}_{0,A}}{4\pi \overline{\kappa}_A} \ln \left[(r'_A + N_{x^2-y^2})^2 - l_{Ax}^2 \right]$$

$$\times \left[(r'_A - N_{x^2-y^2})^2 - l_{Ay}^2 \right],$$

(E3a)

$$N_{x^2-y^2} = -\frac{u_{1,A}}{4\pi \overline{\kappa}_A} \ln \frac{(r'_A + N_{x^2-y^2})^2 - l_{Ax}^2}{(r'_A - N_{x^2-y^2})^2 - l_{Ay}^2},$$

(E3b)

$$l_{A,(x,y)} = \frac{l_{\bar{x},B} \mp l_{\bar{y},B}}{\sqrt{2}} \frac{v_2}{u_{2,A}}$$

(E3c)

$$- \frac{\tilde{u}_{2,A}}{4\pi \overline{\kappa}_A} \ln \frac{r'_A \pm N_{x^2-y^2} + l_{A,(x,y)}}{r'_A \pm N_{x^2-y} - l_{A,(x,y)}}$$

(E3d)

(analogously for the B sector). Assuming a weak mixing $v_0 \ll u_{0,(AB)}$, $v_1 \ll u_{2,(AB)}$, we can expand in orders of $v_{0,1}$. To first order in $v_{0,1}$ we can solve the system by asserting

$l = l^{(0)} + l^{(1)}$, $\psi = \psi^{(0)} + \psi^{(1)}$, where $l^{(0)}$, $\psi^{(0)}$ are solutions to the uncoupled case $v_{0,1} = 0$. To first order

$$\psi_A^{(1)}\left(1 + \frac{u_{0,A}}{4\pi\bar{\kappa}_A}\chi_{A,\Sigma Q}\right)$$

$$= \psi_B^{(0)}\frac{v_0}{u_{0,B}} - \frac{u_{0,A}}{4\pi\bar{\kappa}_A}\Big[\chi_{A,Q_1}(0)\big(N_{x^2-y^2}^{(1)} + l_{A,x}^{(1)}\big)$$

$$+ \chi_{A,-Q_1}(0)\big(N_{x^2-y^2}^{(1)} - l_{A,x}^{(1)}\big)$$

$$- \chi_{A,Q_2}(0)\big(N_{x^2-y^2}^{(1)} - l_{A,y}^{(1)}\big) - \chi_{A,-Q_2}(0)\big(N_{x^2-y^2}^{(1)} + l_{A,y}^{(1)}\big)\Big],$$

$$\text{(E4a)}$$

$$N_{x^2-y^2}^{(1)}\left(1 + \frac{u_{1,A}}{4\pi\bar{\kappa}_A}\chi_{A,\Sigma Q}\right)$$

$$= -\frac{u_{1,A}}{4\pi\bar{\kappa}_A}\Big[\chi_{A,Q_1}(0)\big(\psi_A^{(1)} + l_{A,x}^{(1)}\big)$$

$$+ \chi_{A,-Q_1}(0)\big(\psi_A^{(1)} - l_{A,x}^{(1)}\big) - \chi_{A,Q_2}(0)\big(\psi_A^{(1)} + l_{A,y}^{(1)}\big)$$

$$- \chi_{A,-Q_2}(0)\big(\psi_A^{(1)} - l_{A,y}^{(1)}\big)\Big],$$

$$\text{(E4b)}$$

$$l_{Ax}^{(1)}\left(1 + \frac{u_{2,A}}{4\pi\bar{\kappa}_A}\chi_{A,\Sigma Q_1}\right)$$

$$= \frac{l_{B\bar{x}}^{(0)} - l_{B\bar{y}}^{(0)}}{\sqrt{2}}\frac{v_2}{u_{2,A}}$$

$$- \frac{u_{2,A}}{4\pi\bar{\kappa}_A}(\chi_{A,Q_1}(0) - \chi_{A,-Q_1}(0))\big(\psi_A^{(1)} + N_{x^2-y^2}^{(1)}\big),$$

$$\text{(E4c)}$$

$$l_{Ay}^{(1)}\left(1 + \frac{u_{2,A}}{4\pi\bar{\kappa}_A}\chi_{A,\Sigma Q_2}\right)$$

$$= \frac{l_{B\bar{x}}^{(0)} + l_{B\bar{y}}^{(0)}}{\sqrt{2}}\frac{v_2}{u_{2,A}}$$

$$- \frac{u_{2,A}}{4\pi\bar{\kappa}_A}(\chi_{A,Q_2}(0) - \chi_{A,-Q_2}(0))\big(\psi_A^{(1)} - N_{x^2-y^2}^{(1)}\big),$$

$$\text{(E4d)}$$

and similar for the B sector. Here we used the static susceptibilities of the unperturbed state (24) and introduced $\chi_{A,\Sigma Q} = \chi_{A,Q_1}(0) + \chi_{A,-Q_1}(0) + \chi_{A,Q_2}(0) + \chi_{A,-Q_2}(0)$, $\chi_{A,\Sigma Q_{1,2}} = \chi_{A,Q_{1,2}}(0) + \chi_{A,-Q_{1,2}}(0)$. The correction to the vestigial mean-field solutions because of finite coupling between the sectors is illustrated in Fig. 9, where black
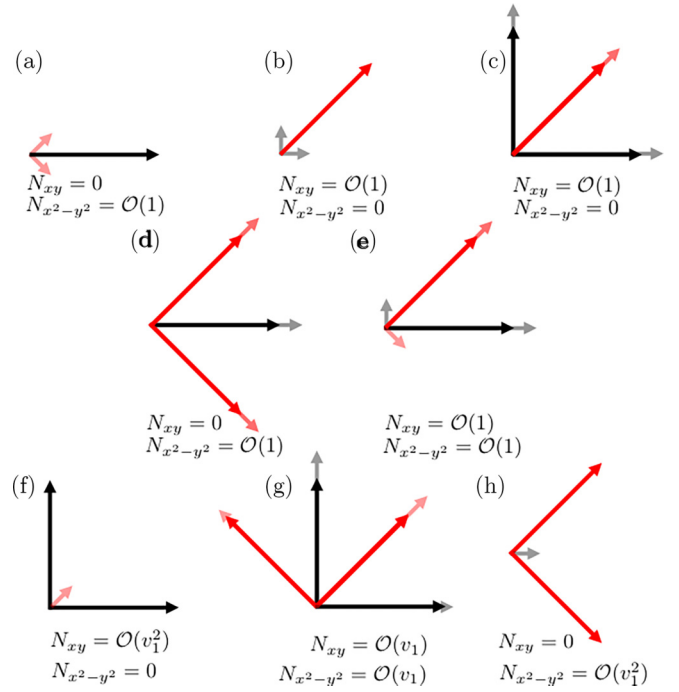

FIG. 9. Effect of couplings between the A and B sectors. Solid black (red) arrows correspond to the unperturbed state in the A (B) sector $v_1 = 0$, whereas the shaded arrows correspond to induced components (first-order in v_1). [(a)–(e)] No additional primary nematic order. [(f)–(h)] Additional primary nematic order is induced.

(red) arrows indicate the LC order in the A (B) sector. In Fig. 9(a) the A sector is ordered in its $x^2 - y^2$ LC state ($l_{A,x} > 0$, $l_{A,y} = 0$), while the B sector is not ordered to zero order in v_1. By turning on the coupling, an LC order in the B sector is induced, $l_{B,x} = l_{B,y} = \mathcal{O}(v_1)$. This state, being symmetric for reflections in the x axis, already has a finite expectation value for the primary nematic field, $N_{x^2-y^2}$, in the unperturbed case [analogous case for the B sector is shown in Fig. 9(b)]. Similar cases are shown in Figs. 9(c)–9(e), where no additional primary nematic order is induced, since it is present already for $v_1 = 0$.

In contrast, for the case noted above, an xy LC phase in the A sector, which only has subleading xy nematic order, $l_{A,x}l_{A,y}$, the coupling will induce a primary xy nematic N_{xy} (stemming from the B sector). This is depicted in Fig. 9(f) [and similarly in Figs. 9(g) and 9(h)].

[1] E. Fradkin, S. A. Kivelson, and J. M. Tranquada, Colloquium: Theory of intertwined orders in high temperature superconductors, Rev. Mod. Phys. **87**, 457 (2015).

[2] J. M. Tranquada, B. J. Sternlieb, J. D. Axe, Y. Nakamura, and S. Uchida, Evidence for stripe correlations of spins and holes in copper oxide superconductors, Nature (London) **375**, 561 (1995).

[3] G. Ghiringhelli, M. Le Tacon, M. Minola, S. Blanco-Canosa, C. Mazzoli, N. B. Brookes, G. M. De Luca, A. Frano, D. G. Hawthorn, F. He *et al.*, Long-range incommensurate charge fluctuations in (Y,Nd)Ba$_2$Cu$_3$O$_{6+x}$, Science **337**, 821 (2012).

[4] J. Chang, E. Blackburn, A. T. Holmes, N. B. Christensen, J. Larsen, J. Mesot, R. Liang, D. A. Bonn, W. N. Hardy, A. Watenphul *et al.*, Direct observation of competition between superconductivity and charge density wave order in YBa$_2$Cu$_3$O$_{6.67}$, Nat. Phys. **8**, 871 (2012).

[5] M. Le Tacon, A. Bosak, S. M. Souliou, G. Dellea, T. Loew, R. Heid, K. P. Bohnen, G. Ghiringhelli, M. Krisch, and B. Keimer, Inelastic x-ray scattering in YBa$_2$Ca$_3$O$_{6.6}$ reveals giant phonon anomalies and elastic central peak due to charge-density-wave formation, Nat. Phys. **10**, 52 (2014).

[6] B. Keimer, S. A. Kivelson, M. R. Norman, S. Uchida, and J. Zaanen, From quantum matter to high-temperature superconductivity in copper oxides, Nature (London) **518**, 179 (2015).

[7] M. J. Lawler, K. Fujita, J. Lee, A. R. Schmidt, Y. Kohsaka, C. K. Kim, H. Eisaki, S. Uchida, J. C. Davis, J. P. Sethna *et al.*, Intra-unit-cell electronic nematicity of the high-T_c copper-oxide pseudogap states, Nature (London) **466**, 347 (2010).

[8] K. Fujita, C. K. Kim, I. Lee, J. Lee, M. H. Hamidian, I. A. Firmo, S. Mukhopadhyay, H. Eisaki, S. Uchida, M. J. Lawler *et al.*, Simultaneous transitions in cuprate momentum-space topology and electronic symmetry breaking, Science **344**, 612 (2014).

[9] Y. Zheng, Y. Fei, K. Bu, W. Zhang, Y. Ding, X. Zhou, J. E. Hoffman, and Y. Yin, The study of electronic nematicity in an overdoped $(Bi, Pb)_2Sr_2CuO_{6+\delta}$ superconductor using scanning tunneling spectroscopy, Sci. Rep. **7**, 8059 (2017).

[10] E. Wahlberg, R. Arpaia, G. Seibold, M. Rossi, R. Fumagalli, E. Trabaldo, N. B. Brookes, L. Braicovich, S. Caprara, U. Gran, G. Ghiringhelli, T. Bauch, and F. Lombardi, Restored strange metal phase through suppression of charge density waves in underdoped $YBa_2Cu_3O_{7-\delta}$, Science **373**, 1506 (2021).

[11] D. F. Agterberg, J. S. Davis, S. D. Edkins, E. Fradkin, D. J. Van Harlingen, S. A. Kivelson, P. A. Lee, L. Radzihovsky, J. M. Tranquada, and Y. Wang, The physics of pair-density waves: Cuprate superconductors and beyond, Annu. Rev. Condens. Matter Phys. **11**, 231 (2020).

[12] A. Himeda, T. Kato, and M. Ogata, Stripe States with Spatially Oscillating d-Wave Superconductivity in the Two-Dimensional t-t'-J Model, Phys. Rev. Lett. **88**, 117001 (2002).

[13] P. Fulde and R. A. Ferrell, Superconductivity in a strong spin-exchange field, Phys. Rev. **135**, A550 (1964).

[14] A. I. Larkin and I. U. N. Ovchinnikov, Inhomogeneous state of superconductors (Production of superconducting state in ferromagnet with Fermi surfaces, examining Green function), Sov. Phys. JETP **20**, 762 (1965).

[15] E. Berg, E. Fradkin, E-A. Kim, S. A. Kivelson, V. Oganesyan, J. M. Tranquada, and S. C. Zhang, Dynamical Layer Decoupling in a Stripe-Ordered High-T_c Superconductor, Phys. Rev. Lett. **99**, 127003 (2007).

[16] E. Berg, E. Fradkin, and S. A. Kivelson, Theory of the striped superconductor, Phys. Rev. B **79**, 064515 (2009).

[17] A. R. Moodenbaugh, Y. Xu, M. Suenaga, T. J. Folkerts, and R. N. Shelton, Superconducting properties of $La_{2-x}Ba_xCuO_4$, Phys. Rev. B **38**, 4596 (1988).

[18] Q. Li, M. Hücker, G. D. Gu, A. M. Tsvelik, and J. M. Tranquada, Two-Dimensional Superconducting Fluctuations in Stripe-Ordered $La_{1.875}Ba_{0.125}CuO_4$, Phys. Rev. Lett. **99**, 067001 (2007).

[19] L. Li, Y. Wang, S. Komiya, S. Ono, Y. Ando, G. D. Gu, and N. P. Ong, Diamagnetism and Cooper pairing above T_c in cuprates, Phys. Rev. B **81**, 054510 (2010).

[20] S. Chakravarty, R. B. Laughlin, D. K. Morr, and C. Nayak, Hidden order in the cuprates, Phys. Rev. B **63**, 094503 (2001).

[21] P. A. Lee, Amperean Pairing and the Pseudogap Phase of Cuprate Superconductors, Phys. Rev. X **4**, 031017 (2014).

[22] S. Baruch and D. Orgad, Spectral signatures of modulated d-wave superconducting phases, Phys. Rev. B **77**, 174502 (2008).

[23] M. Zelli, C. Kallin, and A. J. Berlinsky, Mixed state of a π-striped superconductor, Phys. Rev. B **84**, 174525 (2011).

[24] M. R. Norman and J. C. S. Davis, Quantum oscillations in a biaxial pair density wave state, Proc. Natl. Acad. Sci. USA **115**, 5389 (2018).

[25] Y. Caplan and D. Orgad, Quantum oscillations from a pair-density wave, Phys. Rev. Res. **3**, 023199 (2021).

[26] M. H. Hamidian, S. D. Edkins, S. H. Joo, A. Kostin, H. Eisaki, S. Uchida, M. J. Lawler, E-A. Kim, A. P. Mackenzie, K. Fujita *et al.*, Detection of a Cooper-pair density wave in $Bi_2Sr_2CaCu_2O_{8+x}$, Nature (London) **532**, 343 (2016).

[27] S. D. Edkins, A. Kostin, K. Fujita, A. P. Mackenzie, H. Eisaki, S. Uchida, S. Sachdev, M. J. Lawler, E-A. Kim, J. C. Davis *et al.*, Magnetic field–induced pair density wave state in the cuprate vortex halo, Science **364**, 976 (2019).

[28] A. Kaminski, S. Rosenkranz, H. M. Fretwell, J. C. Campuzano, Z. Li, H. Raffy, W. G. Cullen, H. You, C. G. Olson, C. M. Varma *et al.*, Spontaneous breaking of time-reversal symmetry in the pseudogap state of a high-T_c superconductor, Nature (London) **416**, 610 (2002).

[29] B. Fauqué, Y. Sidis, V. Hinkov, S. Pailhes, C. T. Lin, X. Chaud, and P. Bourges, Magnetic Order in the Pseudogap Phase of High-T_c Superconductors, Phys. Rev. Lett. **96**, 197001 (2006).

[30] Y. Li, V. Balédent, N. Barišić, Y. Cho, B. Fauqué, Y. Sidis, G. Yu, X. Zhao, P. Bourges, and M. Greven, Unusual magnetic order in the pseudogap region of the superconductor $HgBa_2CuO_{4+\delta}$, Nature (London) **455**, 372 (2008).

[31] Y. Li, V. Balédent, N. Barišić, Y. C. Cho, Y. Sidis, G. Yu, X. Zhao, P. Bourges, and M. Greven, Magnetic order in the pseudogap phase of $HgBa_2CuO_{4+\delta}$ studied by spin-polarized neutron diffraction, Phys. Rev. B **84**, 224508 (2011).

[32] Y. Sidis and P. Bourges, Evidence for intra-unit-cell magnetic order in the pseudo-gap state of high-T_c cuprates, J. Phys.: Conf. Ser. **449**, 012012 (2013).

[33] L. Mangin-Thro, Y. Sidis, P. Bourges, S. De Almeida-Didry, F. Giovannelli, and I. Laffez-Monot, Characterization of the intra-unit-cell magnetic order in $Bi_2Sr_2CaCu_2O_{8+\delta}$, Phys. Rev. B **89**, 094523 (2014).

[34] C. M. Varma, Proposal for an experiment to test a theory of high-temperature superconductors, Phys. Rev. B **61**, R3804 (2000).

[35] M. E. Simon and C. M. Varma, Detection and Implications of a Time-Reversal Breaking State in Underdoped Cuprates, Phys. Rev. Lett. **89**, 247003 (2002).

[36] C. M. Varma, Theory of the pseudogap state of the cuprates, Phys. Rev. B **73**, 155113 (2006).

[37] J. Orenstein, Optical Nonreciprocity in Magnetic Structures Related to High-T_c Superconductors, Phys. Rev. Lett. **107**, 067002 (2011).

[38] V. M. Yakovenko, Tilted loop currents in cuprate superconductors, Phys. B: Condens. Matter **460**, 159 (2015).

[39] R. M. Fernandes, A. V. Chubukov, J. Knolle, I. Eremin, and J. Schmalian, Preemptive nematic order, pseudogap, and orbital order in the iron pnictides, Phys. Rev. B **85**, 024534 (2012).

[40] R. M. Fernandes, A. V. Chubukov, and J. Schmalian, What drives nematic order in iron-based superconductors? Nat. Phys. **10**, 97 (2014).

[41] R. M. Fernandes, P. P. Orth, and J. Schmalian, Intertwined vestigial order in quantum materials: Nematicity and beyond, Annu. Rev. Condens. Matter Phys. **10**, 133 (2019).

[42] V. Stanev and Z. Tešanović, Three-band superconductivity and the order parameter that breaks time-reversal symmetry, Phys. Rev. B **81**, 134522 (2010).

[43] T. A. Bojesen, E. Babaev, and A. Sudbø, Time reversal symmetry breakdown in normal and superconducting states in frustrated three-band systems, Phys. Rev. B **88**, 220511(R) (2013).

[44] T. A. Bojesen, E. Babaev, and A. Sudbø, Phase transitions and anomalous normal state in superconductors with broken time-reversal symmetry, Phys. Rev. B **89**, 104509 (2014).

[45] M. Zeng, L.-H. Hu, H.-Y. Hu, Y.-Z. You, and C. Wu, Phase-fluctuation induced time-reversal symmetry breaking normal state, arXiv:2102.06158.

[46] E. Babaev, A. Sudbø, and N. W. Ashcroft, A superconductor to superfluid phase transition in liquid metallic hydrogen, Nature (London) **431**, 666 (2004).

[47] T. Shibauchi, T. Hanaguri, and Y. Matsuda, Exotic superconducting states in FeSe-based materials, J. Phys. Soc. Jpn. **89**, 102002 (2020).

[48] R. M. Fernandes, A. I. Coldea, H. Ding, I. R. Fisher, P. J. Hirschfeld, and G. Kotliar, Iron pnictides and chalcogenides: A new paradigm for superconductivity, Nature (London) **601**, 35 (2022).

[49] C. Cho, J. Shen, J. Lyu, O. Atanov, Q. Chen, S. H. Lee, Y. S. Hor, D. J. Gawryluk, E. Pomjakushina, M. Bartkowiak *et al.*, Z3-vestigial nematic order due to superconducting fluctuations in the doped topological insulators $Nb_xBi_2Se_3$ and $Cu_xBi_2Se_3$, Nat. Commun. **11**, 1 (2020).

[50] S. Mukhopadhyay, R. Sharma, C. K. Kim, S. D. Edkins, M. H. Hamidian, H. Eisaki, Shin-ichi Uchida, E.-A. Kim, M. J. Lawler, A. P. Mackenzie *et al.*, Evidence for a vestigial nematic state in the cuprate pseudogap phase, Proc. Natl. Acad. Sci. USA **116**, 13249 (2019).

[51] V. Grinenko, D. Weston, F. Caglieris, C. Wuttke, C. Hess, T. Gottschall, I. Maccari, D. Gorbunov, S. Zherlitsyn, J. Wosnitza *et al.*, State with spontaneously broken time-reversal symmetry above the superconducting phase transition, Nat. Phys. **17**, 1254 (2021).

[52] L. Nie, G. Tarjus, and S. A. Kivelson, Quenched disorder and vestigial nematicity in the pseudogap regime of the cuprates, Proc. Natl. Acad. Sci. USA **111**, 7980 (2014).

[53] L. Nie, A. V. Maharaj, E. Fradkin, and S. A. Kivelson, Vestigial nematicity from spin and/or charge order in the cuprates, Phys. Rev. B **96**, 085142 (2017).

[54] D. F. Agterberg, D. S. Melchert, and M. K. Kashyap, Emergent loop current order from pair density wave superconductivity, Phys. Rev. B **91**, 054502 (2015).

[55] J. Wårdh and M. Granath, Effective model for a supercurrent in a pair-density wave, Phys. Rev. B **96**, 224503 (2017).

[56] J. Wårdh, B. M. Andersen, and M. Granath, Suppression of superfluid stiffness near a Lifshitz-point instability to finite-momentum superconductivity, Phys. Rev. B **98**, 224501 (2018).

[57] Y.-M. Wu, P. A. Nosov, A. A. Patel, and S. Raghu, Pair Density Wave Order from Electron Repulsion, Phys. Rev. Lett. **130**, 026001 (2023).

[58] J. Wårdh, M. Granath, J. Wu, X. He, and I. Božović, Colossal transverse magnetoresistance due to nematic superconducting phase fluctuations in a copper oxide, arXiv:2203.06769.

[59] V. J. Emery and S. A. Kivelson, Importance of phase fluctuations in superconductors with small superfluid density, Nature (London) **374**, 434 (1995).

[60] Y. J. Uemura, G. M. Luke, B. J. Sternlieb, J. H. Brewer, J. F. Carolan, W. N. Hardy, R. Kadono, J. R. Kempton, R. F. Kiefl, S. R. Kreitzman *et al.*, Universal Correlations between T_c and $\frac{n_s}{m^*}$ (Carrier Density over Effective Mass) in High-T_c Cuprate Superconductors, Phys. Rev. Lett. **62**, 2317 (1989).

[61] J. Wu, A. T. Bollinger, X. He, and I. Božović, Spontaneous breaking of rotational symmetry in copper oxide superconductors, Nature (London) **547**, 432 (2017).

[62] D. F. Agterberg and J. Garaud, Checkerboard order in vortex cores from pair-density-wave superconductivity, Phys. Rev. B **91**, 104512 (2015).

[63] C. Setty, L. Fanfarillo, and P. J. Hirschfeld, Microscopic mechanism for fluctuating pair density wave, arXiv:2110.13138.

[64] C. Setty, J. Zhao, L. Fanfarillo, E. W. Huang, P. J. Hirschfeld, P. W. Phillips, and K. Yang, Exact solution for finite center-of-mass momentum cooper pairing, arXiv:2209.10568.

[65] E.g., for a local interaction $U(\mathbf{q}_1, \mathbf{q}_2, \mathbf{q}_3, \mathbf{q}_4) = U\delta(\mathbf{q}_1 - \mathbf{q}_2 + \mathbf{q}_3 - \mathbf{q}_4)$ we find $u_0 = 7U/4$, $u_1 = -U/4$, $u_2 = -U/2$.

[66] E. Berg, E. Fradkin, and S. A. Kivelson, Charge-4e superconductivity from pair-density-wave order in certain high-temperature superconductors, Nat. Phys. **5**, 830 (2009).

[67] M. Hecker and J. Schmalian, Vestigial nematic order and superconductivity in the doped topological insulator $Ca_xBi_2Se_3$, npj Quantum Mater. **3**, 26 (2018).

[68] I. Božović, X. He, A. T. Bollinger, and R. Caruso, Is nematicity in cuprates real? Condens. Matter **8**, 7 (2023).

[69] Only considering the A sector we do not find any primary (N_{xy}) B_{2g} nematic order, as discussed in Sec. IV A.

[70] Care must be taken when expressing the energy solely in terms of l_x, l_y (see end of Appendix C).

[71] V. Oganesyan, S. A. Kivelson, and E. Fradkin, Quantum theory of a nematic Fermi fluid, Phys. Rev. B **64**, 195109 (2001).

[72] H. Watanabe and A. Vishwanath, Criterion for stability of Goldstone modes and Fermi liquid behavior in a metal with broken symmetry, Proc. Natl. Acad. Sci. USA **111**, 16314 (2014).

[73] C. M. Varma, P. B. Littlewood, S. Schmitt-Rink, E. Abrahams, and A. E. Ruckenstein, Phenomenology of the Normal State of Ca-O High-Temperature Superconductors, Phys. Rev. Lett. **63**, 1996 (1989).

[74] W. Chen, W. Ren, N. Kennedy, M. H. Hamidian, Shin-ichi Uchida, H. Eisaki, P. D. Johnson, S. M. O'Mahony, and J. C. S. Davis, Identification of a nematic pair density wave state in $Bi_2Sr_2CaCu_2O_{8+x}$, Proc. Natl. Acad. Sci. USA **119**, e2206481119 (2022).